

Probabilistic Best Subset Selection via Gradient-Based Optimization

Mingzhang Yin *
mingzhang.yin@columbia.edu

Nhat Ho †
minhnhat@utexas.edu

Bowei Yan ‡
yanbowei@gmail.com

Xiaoning Qian §
xqian@ece.tamu.edu

Mingyuan Zhou †
mingyuan.zhou@mcombs.utexas.edu

June 2, 2022

Abstract

In high-dimensional statistics, variable selection recovers the latent sparse patterns from all possible covariate combinations. This paper proposes a novel optimization method to solve the exact L_0 -regularized regression problem, which is also known as the best subset selection. We reformulate the optimization problem from a discrete space to a continuous one via probabilistic reparameterization. The new objective function is differentiable but its gradient often cannot be computed in a closed form. Then we propose a family of unbiased gradient estimators to optimize the best subset selection objectives by the stochastic gradient descent. Within this family, we identify the estimator with uniformly minimum variance. Theoretically, we study the general conditions under which the method is guaranteed to converge to the ground truth in expectation. The proposed method can find the true regression model from thousands of covariates in seconds. In a wide variety of synthetic and semi-synthetic data, the proposed method outperforms existing variable selection tools based on the relaxed penalties, coordinate descent, and mixed integer optimization in both sparse pattern recovery and out-of-sample prediction.

1 Introduction

Variable selection by regularized regression is widely applied to uncover sparse structures in high dimensional data. It is a natural approach to solving a regression problem with the constraints on the L_0 -norm of the coefficients, as it directly regularizes the number of variables included in the regression model. This is known as the best subset selection problem [Friedman et al., 2001, Fan and Lv, 2010]. In this paper, we study L_0 -regularized regression with the following optimization objective function

$$\min_{\boldsymbol{\beta} \in \mathbb{R}^p} \left\{ \frac{1}{n} \|\mathbf{y} - \mathbf{X}\boldsymbol{\beta}\|_2^2 + \lambda \|\boldsymbol{\beta}\|_0 \right\}, \quad (1)$$

where $\mathbf{y} = (y_1, \dots, y_n)^\top \in \mathbb{R}^n$ is a vector of observed response variables for n units, $\mathbf{X} = (\mathbf{x}_1, \dots, \mathbf{x}_n)^\top \in \mathbb{R}^{n \times p}$ is the design matrix, and $\boldsymbol{\beta} \in \mathbb{R}^p$ are the regression coefficients. The L_0 regularization in Eq. (1) is defined as $\|\boldsymbol{\beta}\|_0 := \sum_{j=1}^p \mathbf{1}_{[\beta_j \neq 0]}$ where $\mathbf{1}_{[\cdot]}$ is an indicator function that equals to one if the condition is true and zero

*Columbia University

†The University of Texas at Austin

‡Independent Researcher

§Texas A&M University

otherwise. This regularization counts the number of nonzero elements. We consider the high-dimensional regime, where the number of covariates p exceeds the sample size n , and can potentially grow with n .

The best subset selection objective in Eq. (1) is nonconvex and is discontinuous with respect to the coefficient β , which is an NP-hard problem to solve [Natarajan, 1995]. A widely used approach to improving the computational efficiency is to approximate the L_0 -norm with continuous regularizations. As a pioneer framework, the Bridge regression [Frank and Friedman, 1993, Fu, 1998] considers the L_q penalties ($q > 0$), defined as $\sum_{j=1}^p \beta_j^q$ for the regression coefficient β_j . When $q \geq 1$, the L_q penalty is convex, while when $q \leq 1$, the regularization encourages sparse estimation and hence performs variable selection [Fan and Lv, 2010]. In the intersection of these two domains lies the widely used least absolute shrinkage and selection operator (LASSO). Asymptotically, LASSO is accurate for both sparse pattern recovery and coefficient estimation [Zhao and Yu, 2006, Candès and Plan, 2009, Wainwright, 2009]. However, in the finite sample setting, it introduces downward bias due to the shrinkage effect of the L_1 norm and might select an excessively large subset based on the cross validation in practice [Bertsimas et al., 2016, Hastie et al., 2020].

In this paper, we solve the best subset selection problem directly. Compared to continuous approximations, the solution of the exact best subset selection enjoys superior statistical properties, such as the unbiasedness of regression coefficients, known as the oracle property [Greenshtein, 2006, Zhang and Zhang, 2012, Belloni and Chernozhukov, 2013], and the low in-sample risk [Foster and George, 1994]. For example, Johnson et al. [2015] shows that the predictive risk of the L_1 -regularized linear regression cannot outperform L_0 -regularized regression by more than a small constant factor and in some cases is infinitely worse under assumptions of the design matrix.

Thanks to the benefits of L_0 penalty and the fast improvements in modern computational tools, recently there is renewed interest in solving the exact best subset selection problem. Bertsimas et al. [2016] solve the constrained best subset selection problem

$$\min_{\beta \in \mathbb{R}^p} \left\{ \frac{1}{n} \|\mathbf{y} - \mathbf{X}\beta\|_2^2 \right\} \quad \text{subject to} \quad \|\beta\|_0 \leq \hat{S} \quad (2)$$

with a two-stage algorithm using mixed integer optimization (MIO). MIO methods scale up the number of covariates p for the best subset selection from 30s to 1000s [Furnival and Wilson, 1974, Bertsimas et al., 2016]. However, the MIO steps rely upon a nonconvex optimization tool such as Gurobi [Gurobi Optimization, LLC, 2022], which is not straightforward to generalize beyond linear regression problems. Moreover, solving Eq. (2) exactly with an MIO algorithm might be computationally expensive [Gómez and Prokopyev, 2021]. The computational efficiency of the MIO method is improved by searching a hierarchy of local minima of the objective function in Eq. (1) with coordinate descent and local combinatorial search [Hazimeh and Mazumder, 2018].

This paper proceeds in the direction of solving the best subset selection by providing a gradient-based solution. We first propose a probabilistic objective for the exact L_0 -regularized regression by casting the discrete optimization problem to an equivalent one in the continuous space. The new objective function is differentiable, but the exact gradient is infeasible to compute in practice when the covariates are high dimensional. Then, we propose a family of unbiased estimators to approximate the infeasible gradient. Within this unbiased estimator family, we identify the estimator with minimal variance and a non-vanishing signal-to-noise ratio. By construction, the gradient estimators are computationally efficient in high dimensions. The result is an end-to-end solver for the best subset selection with the modern stochastic gradient descent (SGD) as the main workhorse. We provide theoretical insights on the conditions that guarantee the convergence of the gradient descent updates to the ground truth in expectation.

The proposed gradient method has several strengths. First, it scales to practical problems with high dimensional covariates. The exact gradient can be estimated accurately with a few random samples, and the algorithm searches for the best subset in the steepest descent direction of the objective function. Second, the gradient method has high flexibility. Aside from the regularized regression objective in Eq. (1), we further apply the gradient method to solve a new variational objective for the Bayesian linear regression with the spike-and-slab prior [Mitchell and Beauchamp, 1988]. Empirically, compared to existing variable selection methods with continuous relaxation and L_0 penalties, we find the gradient-based method improves the sparsity pattern recovery, the coefficient estimation, and out-of-sample prediction across a wide range of problem settings.

Related work. A major paradigm in variable selection is based on continuous penalties. In addition to the Bridge regression we have discussed, there are a variety of nonconvex penalties for sparsity learning. Smoothly clipped absolute deviation (SCAD) [Fan and Li, 2001] and minimax concave penalty (MCP) [Zhang, 2010], for example, approximate the hard-thresholding property of L_0 regularizer by the piece-wise nonconvex functions. Some work construct penalties to directly resemble the functional form of the L_0 penalty, known as the pseudo- L_0 penalties [Liu and Wu, 2007, Shen et al., 2012, Dicker et al., 2013]. Since there is a rich literature on variable selection, we refer readers to several representative publications [Friedman et al., 2001, Fan and Lv, 2010, Bertsimas et al., 2016, Hastie et al., 2020] and the references therein for comprehensive reviews.

The L_0 -regularized subset selection is closely related to the standard information theoretic methods for model selection. In particular, when the data is Gaussian distributed, Eq. (1) is equivalent to the Akaike information criterion (AIC) [Akaike, 1974, 1998] for $\lambda = 1/n$, and is equivalent to the Bayesian information criterion (BIC) [Schwarz, 1978] for $\lambda = \log(n)/(2n)$. The objective function in Eq. (1) incorporates the information criterions directly into the optimization, hence performing model comparison among a wide range of candidate models.

Last, the proposed gradient method is related to the growing field of discrete optimization in machine learning [Mohamed et al., 2020]. These works often consider a latent variable model with Bernoulli or Categorical latent variables, such as the actions in policy learning and the activation layers in belief networks [Gu et al., 2015, Yue et al., 2020]. A variety of variance reduction techniques lie at the core of these discrete optimization methods, such as Gumbel-softmax relaxation [Maddison et al., 2016, Jang et al., 2017], control variates [Tucker et al., 2017], antithetic sampling [Yin and Zhou, 2019], and Gaussian-based continuous relaxation [Yamada et al., 2020]. In spite of empirical success in optimizing neural networks in the areas such as deep generative models and reinforcement learning, the statistical properties of these methods are largely unknown. By studying the best subset selection problem with gradient methods, we systematically analyze the bias-variance trade-off and the convergence properties, and further propose a new discrete optimization tool.

Organization. The remainder of this paper is organized as follows. In Section 2, we provide a probabilistic reformulation of the L_0 -regularized linear regression problem. In Section 3, we propose a family of unbiased gradient estimators to solve the reformulated optimization problem. In Section 4, we analyze the conditions that guarantee the convergence to the ground truth in expectation. In Section 5, we generalize the proposed gradient methods to optimize a novel variational lower bound for the Bayesian best subset selection. Experiments and results are described in Section 6, and discussions follow in Section 7.

Notation. We use n as the sample size, p as the number of covariates, and S as the number of non-zero true coefficients. We use \mathbf{x}_i to denote the i^{th} row of matrix \mathbf{X} and X_j as its j^{th} column. We use $\mathbf{X}_{\mathcal{A}}$ to denote a submatrix of \mathbf{X} as $\mathbf{X}_{\mathcal{A}} = \{X_j\}_{j \in \mathcal{A}}$, $\mathcal{A} \subseteq [p]$, where $[p] := \{1, \dots, p\}$. We assume a constant bias term is contained in the covariate matrix.

2 Reformulation of L_0 -Penalized Regression

The underlying assumption of best subset selection is that the response variables only depend on a subset of covariates $\mathbf{X}_{\mathcal{A}}$, where $\mathcal{A} \subseteq \{1, \dots, p\}$ is called the active set. The true active set S is assumed to be much smaller than p . We decompose the regression coefficients as $\boldsymbol{\beta} = \boldsymbol{\alpha} \odot \mathbf{z}$, using a spike-and-slab construction [George and McCulloch, 1993], where \odot denotes an element-wise product. The binary vector $\mathbf{z} \in \{0, 1\}^p$ represents the inclusion of covariates in the active set, and $\boldsymbol{\alpha} \in \mathbb{R}^p$ encodes the scale. With the augmented latent variables, the optimization problem (1) can be equivalently expressed as

$$\min_{\boldsymbol{\alpha}, \mathbf{z}} \frac{1}{n} \|\mathbf{y} - \mathbf{X}(\boldsymbol{\alpha} \odot \mathbf{z})\|^2 + \lambda \|\mathbf{z}\|_0. \quad (3)$$

Similar to optimizing $\boldsymbol{\beta}$ itself, optimizing \mathbf{z} is a combinatorial problem and remains NP-hard.

A major bottleneck in solving Eq. (3) is the discrete nature of variable \mathbf{z} that precludes computing the gradient with respect to it, which could have provided the direction of the steepest descent. This motivates us to reformulate the discrete optimization problem Eq. (3) to an optimization problem in the continuous

space. Such continuity greenlights the gradient-based methods, the workhorse behind modern machine learning. Specifically, instead of directly optimizing \mathbf{z} , we consider \mathbf{z} as a random variable with distribution $p(\mathbf{z}; \boldsymbol{\pi}) = \prod_{j=1}^p \text{Bern}(z_j; \pi_j)$, $\pi_j \in [0, 1]$, where $\text{Bern}(z_j; \pi_j)$ is the Bernoulli distribution with parameter π_j . Then the problem in Eq. (3) can be transformed to a probabilistic objective in the form of expectation. The new objective function allows us to construct a stochastic gradient with Monte Carlo estimation. We have the following theorem for the reformulation.

Theorem 1 (Probabilistic Reformulation). *The L_0 -regularized best subset selection problem (1) is equivalent to the following problem*

$$\min_{\boldsymbol{\pi}} \mathbb{E}_{\mathbf{z} \sim p(\mathbf{z}; \boldsymbol{\pi})} \left[\min_{\boldsymbol{\alpha}} \frac{1}{n} \|\mathbf{y} - \mathbf{X}(\boldsymbol{\alpha} \odot \mathbf{z})\|_2^2 + \lambda \|\mathbf{z}\|_0 \right], \quad (4)$$

where $\boldsymbol{\pi} = (\pi_1, \pi_2, \dots, \pi_p) \in [0, 1]^p$, $p(z_j = 1) = \pi_j$, $j \in \{1, \dots, p\}$.

The equivalence can be proved by the fact that the optimal solution of Eq. (3) is a feasible solution of Eq. (4) that achieves the same objective value, and vice versa. Though Eq. (4) optimizes over a space larger than that of Eq. (3), the optima of π_j is always at its extremes, *i.e.* either zero or one. By Eq. (3), we relax the optimization from a discrete space to a continuous space. The proof is in Appendix B.1.

The objective in Eq. (4) is a bi-level optimization problem, where the inner optimization for a given \mathbf{z} is an ordinary least square (OLS) problem on the design matrix $\mathbf{X}_{\mathcal{Z}}$, which has a closed-form solution. Denote the active set inferred by \mathbf{z} as $\mathcal{Z} := \{j\}_{j:z_j \neq 0}$. Since the computation of OLS has a cubic-scaling cost with the number of regressors, the computational speed of the inner optimization increases when the size of \mathcal{Z} decreases, *i.e.*, the sparser the faster. Since we assume the true active set size S is small, an algorithm that accurately selects variables can solve the inner optimization efficiently.

For computational convenience, we reparameterize $\boldsymbol{\pi} = (\pi_1, \dots, \pi_p)$ with the sigmoid function as $\pi_j = \sigma(\phi_j) = 1/(1 + \exp(-\phi_j))$, $j \in [p]$ and further relax the optimization space to an unconstrained space. Although under the sigmoid reparameterization, probability π_j can reach 0 or 1 only when the logit ϕ_j goes to the infinity, it can be accurately approximated in practice when the absolute values of the logits ϕ_j are sufficiently large.

A naive approach guaranteed to select the best subset is to exhaust all possible subsets. The exhaustion method is often infeasible because it requires evaluating the function under expectation 2^p times with p covariates. A key to improving computational efficiency is minimizing the number of function evaluations. Instead of a random search, our idea is to guide the function evaluation by the first-order information given by the stochastic gradient. In the following section, we build a family of unbiased gradient estimators in the univariate case, then generalize the estimators to high dimensions.

3 A Family of Unbiased Gradient Estimators

Consider a general probabilistic objective

$$\min_{\boldsymbol{\phi}} \mathcal{E}(\boldsymbol{\phi}) = \mathbb{E}_{\mathbf{z} \sim p_{\boldsymbol{\phi}}(\mathbf{z})} [f(\mathbf{z})], \quad (5)$$

where $p_{\boldsymbol{\phi}}(\mathbf{z}) = \prod_{j=1}^p \text{Bern}(\sigma(\phi_j))$. The L_0 -regularized objective in Eq. (4) is a specific instance of Eq. (5) with function

$$f(\mathbf{z}) = \min_{\boldsymbol{\alpha}} \|\mathbf{y} - \mathbf{X}(\boldsymbol{\alpha} \odot \mathbf{z})\|_2^2 / n + \lambda \|\mathbf{z}\|_0. \quad (6)$$

Taking the gradient of $\mathcal{E}(\boldsymbol{\phi})$ in Eq. (5) with respect to $\boldsymbol{\phi}$, and exchanging the derivative and integral, we have

$$\nabla_{\boldsymbol{\phi}} \mathcal{E}(\boldsymbol{\phi}) = \nabla_{\boldsymbol{\phi}} \mathbb{E}_{\mathbf{z} \sim p_{\boldsymbol{\phi}}(\mathbf{z})} [f(\mathbf{z})] = \mathbb{E}_{\mathbf{z} \sim p_{\boldsymbol{\phi}}(\mathbf{z})} [f(\mathbf{z}) \nabla_{\boldsymbol{\phi}} \log p_{\boldsymbol{\phi}}(\mathbf{z})]. \quad (7)$$

The last equality of Eq. (7) is called the *score method* in statistics [Serfling, 2009] and *REINFORCE* in reinforcement learning (RL) [Williams, 1992]. The expectation in Eq. (7) cannot be computed analytically for high dimensional \mathbf{z} , but it can be approximated by an unbiased Monte Carlo estimation

$\frac{1}{K} \sum_{k=1}^K f(\mathbf{z}_k) \nabla_{\phi} \log p_{\phi}(\mathbf{z}_k)$, with $\mathbf{z}_1, \dots, \mathbf{z}_K \stackrel{iid}{\sim} p_{\phi}(\mathbf{z})$. This approximation is widely used as the policy gradient in RL and robotics [Peters and Schaal, 2006].

The continuous reformulation in Eq. (4) and the score method in Eq. (7) make it possible to solve the best subset selection with gradient descent. One advantage of approximating the gradient in Eq. (7) with Monte Carlo estimation is that the number of function evaluations does not grow with the dimension of variable \mathbf{z} . This property is essential for scaling to high dimensions. Another advantage of the score method is that computing such a gradient estimator only requires the value of function $f(\mathbf{z})$ instead of its derivatives. It is applicable to the situations where $f(\mathbf{z})$ is discontinuous or even has no explicit expression (e.g., in RL, $f(\mathbf{z})$ could be the unknown reward function for action \mathbf{z}).

However, the score function gradient is known for high variance [Greensmith et al., 2004, Jang et al., 2017, Tucker et al., 2017]. Though the Monte Carlo estimation with K samples reduces the variance in the order $\mathcal{O}(1/K)$, it needs many function evaluations for an accurate gradient estimate at each step.

To solve this problem, we develop a general framework for unbiased gradient estimation with variance reduction techniques. We construct a family of unbiased gradient estimators and identify the estimator with minimal variance in this family.

3.1 Insights from univariate gradient setting

We first develop gradient estimators for a univariate latent variable and then generalize them to high dimensional variables. When the variable z in Eq. (5) is a scalar, the analytic gradient is

$$\nabla_{\phi} \mathbb{E}_{z \sim \text{Bern}(\sigma(\phi))} [f(z)] = \sigma(\phi)(1 - \sigma(\phi)) [f(1) - f(0)]. \quad (8)$$

The closed form of expectation above provides an explicit condition that an unbiased gradient estimator must satisfy. To cope with the best subset selection objective in Eq. (4), the gradient estimator should further not rely on the continuity of function $f(\mathbf{z})$, and the number of required function evaluations does not increase with the dimension of the covariates. According to these desiderata, we define a family of gradient estimators.

Definition 1 (Unbiased gradient family). *For an objective $\mathbb{E}_{z \sim \text{Bern}(\sigma(\phi))} [f(z)]$, suppose an estimator of the gradient with respect to ϕ is in the form of $g(u; \sigma(\phi))$ where $u \sim \text{Unif}(0, 1)$ is a uniform random variable. For function $f : \{0, 1\} \rightarrow \mathbb{R}$, the unbiased gradient family \mathcal{G} consists of function $g(u; \sigma(\phi))$ that satisfies*

- *Unbiasedness:* $\mathbb{E}_{u \sim \text{Unif}(0,1)} [g(u; \sigma(\phi))] = \sigma(\phi)(1 - \sigma(\phi)) [f(1) - f(0)]$,
- *Functional form:*

$$g(u; \sigma(\phi)) = a(u; \sigma(\phi)) f(\mathbf{1}_{[u < \sigma(\phi)]}) + b(u; \sigma(\phi)) f(\mathbf{1}_{[u > 1 - \sigma(\phi)]}) \quad (9)$$

where $a(u; \sigma(\phi))$, $b(u; \sigma(\phi))$ are independent of function $f(\cdot)$.

The gradient family \mathcal{G} in Definition 1 is a set of unbiased gradient estimators with a specific functional form in Eq. (9). This functional form ensures efficiency when generalizing to the high dimensional settings, which will be discussed in detail in Section 3.2. The estimator family \mathcal{G} with this functional form incorporates many popular unbiased gradient estimators. Here we list several representative ones.

The REINFORCE estimator belongs to the family \mathcal{G} with

$$g_R(u; \sigma(\phi)) = f(\mathbf{1}_{[u < \sigma(\phi)]}) (\mathbf{1}_{[u < \sigma(\phi)]} - \sigma(\phi)). \quad (10)$$

A recently proposed ARM gradient [Yin and Zhou, 2019] is an element of \mathcal{G} with

$$g_{\text{ARM}}(u; \sigma(\phi)) = [f(\mathbf{1}_{[u > 1 - \sigma(\phi)]}) - f(\mathbf{1}_{[u < \sigma(\phi)]})] (u - \frac{1}{2}). \quad (11)$$

We can add an indicator mask to the ARM gradient without changing its univariate distribution, which we call it ARM_0 estimator, with the expression as

$$g_{\text{ARM}_0}(u; \sigma(\phi)) = [f(\mathbf{1}_{[u > \sigma(-\phi)]}) - f(\mathbf{1}_{[u < \sigma(\phi)]})] (u - \frac{1}{2}) \mathbf{1}_{[u > \sigma(-\phi)]} - \mathbf{1}_{[u < \sigma(\phi)]}. \quad (12)$$

	REINFORCE	ARM	ARM ₀	U2G
$a(u; \sigma(\phi))$	$\mathbf{1}_{[u < \sigma(\phi)]} - \sigma(\phi)$	$\frac{1}{2} - u$	$(\frac{1}{2} - u) \mathbf{1}_{[u > \sigma(-\phi)]} - \mathbf{1}_{[u < \sigma(\phi)]} $	$\sigma(\phi)(\mathbf{1}_{[u < \sigma(\phi)]} - \mathbf{1}_{[u > \sigma(-\phi)])}/2$
$b(u; \sigma(\phi))$	0	$u - \frac{1}{2}$	$(u - \frac{1}{2}) \mathbf{1}_{[u > \sigma(-\phi)]} - \mathbf{1}_{[u < \sigma(\phi)]} $	$\sigma(\phi)(\mathbf{1}_{[u > \sigma(-\phi)]} - \mathbf{1}_{[u < \sigma(\phi)]})/2$

Table 1: Parameterization of unbiased gradient estimators according to Definition 1.

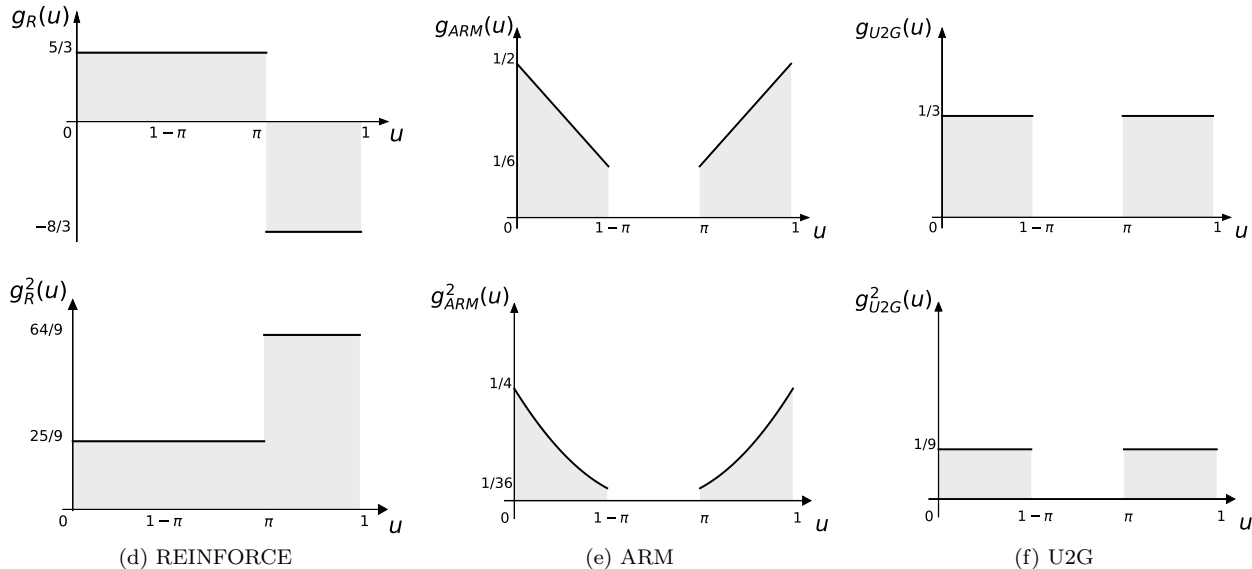


Figure 1: The characteristic curves of gradient estimators. In this illustrative example, $f(1) = 5$, $f(0) = 4$, and $\pi = \sigma(\phi) = 2/3$. The top row is the function $g(u)$ with respect to u ; the second row is the function $g^2(u)$. The unbiased estimators have the same integration in the first row, but different gradient variance as shown in the second row (up to a constant).

In the univariate case, the ARM₀ estimator is identical to the ARM estimator, but when it comes to the multivariate case, ARM₀ can produce sparse gradients where many elements may become exact zeros. This straightforward sparsification of the ARM estimator has been adopted by several recent works [Boluki et al., 2020, Yue et al., 2020, Dadaneh et al., 2020].

In this paper, we propose a new gradient estimator that can further reduce the variance, which is given by

$$g_{U2G}(u; \sigma(\phi)) = \frac{\sigma(|\phi|)}{2} [f(\mathbf{1}_{[u > 1 - \sigma(\phi)])} - f(\mathbf{1}_{[u < \sigma(\phi)])}] (\mathbf{1}_{[u > \sigma(-\phi)]} - \mathbf{1}_{[u < \sigma(\phi)]}). \quad (13)$$

We call it unbiased uniform gradient (U2G) estimator because it takes a constant value at the non-zero region. U2G estimator is derived by finding the minimum-variance unbiased estimator (MVUE) from the family in Definition 1; Section 3.1.1 will discuss the derivation in detail. U2G estimator is concurrently discovered by Dong et al. [2020] via Rao-Blackwellization over the ARM estimator and exhibits promising performance in optimizing neural network parameters of deep generative models. We summarize the estimators above in Table 1 in a functional form compatible with Definition 1.

We are interested in the bias-variance behavior of the gradient estimators. The estimators of the family \mathcal{G} are unbiased thus having the same expectation value. But the variance differs between them, depending on how the estimator is expressed as a function $g(u; \sigma(\phi))$ of a uniform variable u . As an illustrative example, Figure 1 shows the functions $g(u)$ and $g^2(u)$ for the estimators in Eqs. (10), (11) and (13) with $f(1) = 5$, $f(0) = 4$, and $\pi = \sigma(\phi) = 2/3$. Since the estimators are unbiased, the net signed areas under the curve of the first row in Figure 1 are the same. The variance of each gradient estimator, up to the same additive constant, is represented by the area under the curve in each subplot of the second row.

Compare the first column of Figure 1 to the other two columns, and compare Eq. (10) to Eqs. (11) and (13). Intuitively, if the function $f(\cdot)$ appears in the estimator as a relative difference $f(z) - f(z')$, the scale of

the gradient does not increase with the scale of $f(\cdot)$, and the magnitude of the second moment is controlled. The relative difference $f(z) - f(z')$ echos the model comparison nature of variable selection.

Comparing the second and the third columns of Figure 1, intuitively, we find the variance (or the second moment) is reduced if the direction and magnitude of the gradient estimator do not change with variable u . Formally, we have the following result.

Proposition 1. *For positive (or negative) function $f(z)$, i.e. $f(z) \geq 0$, we have*

$$\text{var}[g_{\text{U2G}}] \leq \text{var}[g_{\text{ARM}}] \leq \text{var}[g_{\text{R}}],$$

where the second inequality requires $|f(1) - f(0)| \leq \min\{|f(1)|, |f(0)|\}$.

The proof of Proposition 1 is presented in Appendix B.2.

3.1.1 Optimality of U2G estimator

We derive U2G estimator by identifying the estimator with minimal variance in the family \mathcal{G} in Definition 1. To simplify the notation, let $f_1 = f(1)$, $f_0 = f(0)$, $\pi = \sigma(\phi)$, and $\Delta = |f_0 - f_1|$. Without loss of generality, we assume $\pi \geq 1/2$. An ideal gradient for variable selection should be able to distinguish the potential models, even when their difference is small. Accordingly, a gradient estimator should have a non-diminishing SNR, defined as $\text{SNR} := \mathbb{E}[g(u)] / \sqrt{\text{var}[g(u)]}$.

However, as shown in Eq. (8), the scale of the true gradient diminishes as the difference Δ between the potential models shrinks. For a non-diminishing SNR, the variance of the estimator $g(u)$ has to decrease to zero as $\Delta \rightarrow 0$, that is

$$\lim_{\Delta \rightarrow 0} \text{var}[g(u; \pi)] = 0, \quad \text{for all } \pi. \quad (14)$$

This condition ensures the estimated gradient can distinguish the optimal model from the others, even when the objective values are close.

Under the condition in Eq. (14), the following proposition shows that U2G is the uniformly minimum-variance unbiased estimator (UMVUE) within the proposed estimator family \mathcal{G} . U2G estimator hence has the optimal statistical efficiency. The proof is in Appendix B.3.

Proposition 2. *Among the unbiased gradient estimators defined in Definition 1 and assume $\forall \pi, \lim_{|f(1)-f(0)| \rightarrow 0} \text{var}[g(u; \pi)] = 0$, U2G has the uniformly minimum variance for all π .*

Specifically, for univariate latent variable, the variance of U2G estimator is

$$\begin{aligned} \text{var}[g_{\text{U2G}}(u; \pi)] &= \pi \left| \pi - \frac{1}{2} \right| (1 - \pi) \max\{\pi, 1 - \pi\} [f(1) - f(0)]^2 \\ &\leq C [f(1) - f(0)]^2 \end{aligned}$$

with $C \approx 0.0388$. The SNR for U2G estimator is

$$\text{SNR}(\pi) = \sqrt{\pi(1 - \pi) / \left(\left| \pi - \frac{1}{2} \right| \max\{\pi, 1 - \pi\} \right)},$$

which is the same for arbitrary function $f(\cdot)$ in the objective, and only vanishes when the algorithm converges, i.e. $\pi \rightarrow 0$ or 1. Similar properties hold for the ARM estimator. The variance and SNR of the ARM and U2G estimators are shown in Figure 2. U2G estimator has lower variance and higher SNR than ARM estimator, especially when the Bernoulli probability the uncertainty is high (π is close to 0.5).

3.2 Multivariate Generalization

We generalize the univariate gradient estimators in Section 3.1 to the setting with high dimensional variable \mathbf{z} . When \mathbf{z} is univariate, it is unnecessary to estimate the gradient given the true gradient in Eq. (8).

However, the true gradient is not accessible in the multivariate case. An element of the true gradient vector is

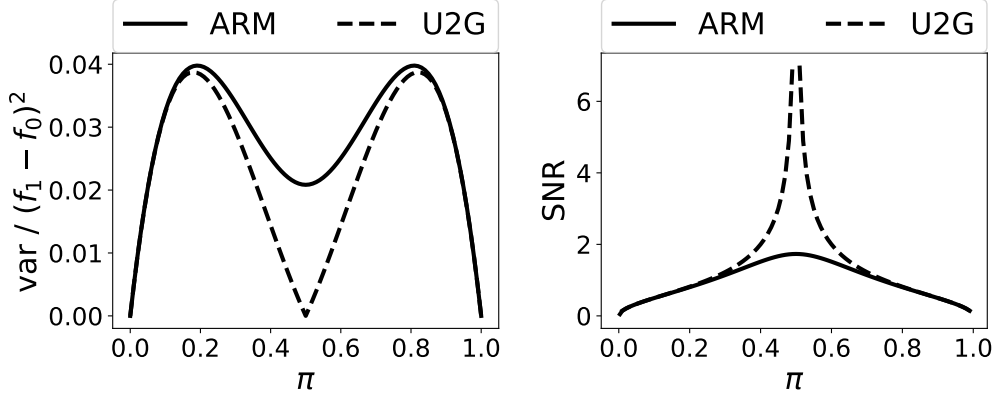


Figure 2: Variance and SNR of univariate ARM and U2G estimators.

$$\begin{aligned} \frac{\partial}{\partial \phi_v} \mathcal{E}(\phi) &= \frac{\partial}{\partial \phi_v} \mathbb{E}_{\mathbf{z} \sim \prod_{j=1}^p p(z_j; \sigma(\phi_j))} [f(\mathbf{z})] \\ &= \mathbb{E}_{\mathbf{z}_{-v}} [\sigma(\phi_v)(1 - \sigma(\phi_v))(f(\mathbf{z}_{-v}, z_v = 1) - f(\mathbf{z}_{-v}, z_v = 0))]. \end{aligned} \quad (15)$$

Estimating the gradient vector element-wisely by Eq. (15) requires high computational cost. To estimate the v -th element with the Monte Carlo method by Eq. (15), we first sample a binary vector \mathbf{z} . Then the function $f(\cdot)$ needs to be computed on two binary vectors with the v -th element as 0 and 1 respectively and other elements equal to \mathbf{z}_{-v} . This has to be done for each element of \mathbf{z} separately. Therefore, it requires at least $2p$ evaluations of function $f(\cdot)$ to get an unbiased gradient estimate at each step. For the best subset selection, the function $f(\cdot)$ in Eq. (6) involves a least square regression on the support set of \mathbf{z} . Hence, evaluating $f(\cdot)$ $2p$ times for each gradient step is computationally intractable for the large- p setting.

The functional form of the estimators in Definition 1 circumvent this computational problem. Applying the univariate gradient estimators in Definition 1, for multivariate \mathbf{z} , an element of the gradient vector can be computed as

$$\begin{aligned} & \frac{\partial}{\partial \phi_v} \mathbb{E}_{\mathbf{z} \sim \prod_{j=1}^p p(z_j; \sigma(\phi_j))} [f(\mathbf{z})] \\ &= \mathbb{E}_{\mathbf{z}_{-v}} \frac{\partial}{\partial \phi_v} \mathbb{E}_{z_v \sim p(z_v; \sigma(\phi_v))} [f(z_v, \mathbf{z}_{-v})] \\ &= \mathbb{E}_{\mathbf{z}_{-v}} \mathbb{E}_{u_v \sim \text{Unif}(0,1)} [a(u_v; \sigma(\phi_v)) f(\mathbf{1}_{[u_v < \sigma(\phi_v)]}, \mathbf{z}_{-v}) + b(u_v; \sigma(\phi_v)) f(\mathbf{1}_{[u_v > 1 - \sigma(\phi_v)]}, \mathbf{z}_{-v})] \\ &= \mathbb{E}_{\mathbf{u} \sim \prod_{j=1}^p \text{Unif}(0,1)} [a(u_v; \sigma(\phi_v)) f(\mathbf{1}_{[\mathbf{u} < \sigma(\phi)]}) + b(u_v; \sigma(\phi_v)) f(\mathbf{1}_{[\mathbf{u} > 1 - \sigma(\phi)]})]. \end{aligned} \quad (16)$$

The first equality is by the factorization of $p(\mathbf{z})$, the second equality is by the unbiasedness of the univariate gradient estimator form in Definition 1, and the last equality is by the law of the unconscious statistician (LOTUS) [Ross, 2014]. Eq. (16) ensures that

$$\mathbf{g}(\mathbf{u}; \sigma(\phi)) = a(u_v; \sigma(\phi_v)) f(\mathbf{1}_{[\mathbf{u} < \sigma(\phi)]}) + b(u_v; \sigma(\phi_v)) f(\mathbf{1}_{[\mathbf{u} > 1 - \sigma(\phi)]}), \quad \mathbf{u} \sim \prod_{j=1}^p \text{Unif}(0, 1), \quad (17)$$

is an unbiased estimator for the gradient of the objective Eq. (5).

The estimator in Eq. (17) has a key computational advantage. We can evaluate $f(\mathbf{1}_{[\mathbf{u} < \sigma(\phi)]})$ and $f(\mathbf{1}_{[\mathbf{u} > 1 - \sigma(\phi)]})$ as few as a single time with $\mathbf{u} \sim \prod_{j=1}^p \text{Unif}(0, 1)$, and share it across all the elements of the gradient vector, greatly reducing computational time.

Written in a vector form, the estimators in Section 3.1 have their multivariate form as

$$\begin{aligned} \mathbf{g}_R(\mathbf{u}; \sigma(\phi)) &= f(\mathbf{1}_{[\mathbf{u} < \sigma(\phi)]}) (\mathbf{1}_{[\mathbf{u} < \sigma(\phi)]} - \sigma(\phi)), \\ \mathbf{g}_{\text{ARM}_0}(\mathbf{u}; \sigma(\phi)) &= [f(\mathbf{1}_{[\mathbf{u} > 1 - \sigma(\phi)]}) - f(\mathbf{1}_{[\mathbf{u} < \sigma(\phi)]})] (\mathbf{u} - \frac{1}{2}) \odot |\mathbf{1}_{[\mathbf{u} > 1 - \sigma(\phi)]} - \mathbf{1}_{[\mathbf{u} < \sigma(\phi)]}|, \end{aligned}$$

Algorithm 1 Best subset selection with probabilistic reformulation

input : Bernoulli distribution $\{q_{\phi_j}(z_j)\}_{j \in [p]}$ with probability $\{\sigma(\phi_j)\}_{j \in [p]}$, target $\mathcal{E}(\phi) = \mathbb{E}_{\mathbf{z} \sim p_\phi(\mathbf{z})}[f(\mathbf{z})]$, $\mathbf{z} = (z_1, \dots, z_p)$, $\phi = (\phi_1, \dots, \phi_p)$, $p_\phi(\mathbf{z}) = \prod_{j=1}^p p_{\phi_j}(z_j)$
output: Maximum likelihood estimator of $p_\phi(\mathbf{z})$ as $\hat{\mathbf{z}} = \mathbf{1}_{[\sigma(\phi) > 1/2]}$

Initialize ϕ randomly

while *not converged* **do**

 Sample $\mathbf{u}_k \stackrel{i.i.d.}{\sim} \prod_{j=1}^p \text{Unif}(0, 1)$ for $k = 1, \dots, K$
 Evaluate $f(\mathbf{1}_{[\mathbf{u}_k > 1 - \sigma(\phi)]})$ and $f(\mathbf{1}_{[\mathbf{u}_k < \sigma(\phi)]})$
 Compute $\mathbf{g}_k = g(\mathbf{u}_k; \sigma(\phi), f)$ by an estimator in Eq. (18)
 Update $\phi = \phi - \frac{1}{K} \rho \sum_{k=1}^K \mathbf{g}_k$ with stepsizes ρ

end

$$\mathbf{g}_{\text{U2G}}(\mathbf{u}; \sigma(\phi)) = \frac{1}{2} [f(\mathbf{1}_{[\mathbf{u} > 1 - \sigma(\phi)]}) - f(\mathbf{1}_{[\mathbf{u} < \sigma(\phi)]})] \sigma(|\phi|) \odot (\mathbf{1}_{[\mathbf{u} > 1 - \sigma(\phi)]} - \mathbf{1}_{[\mathbf{u} < \sigma(\phi)]}), \quad (18)$$

where $\mathbf{u} \sim \prod_{j=1}^p \text{Unif}(0, 1)$, and all the operations are element-wise. Due to the indicator mask, the gradient vectors of ARM₀ and U2G are sparse when the probability close to the extremes such as when the algorithm is close to the convergence. We observe in practice that the sparsity in gradient estimation, while not required to ensure unbiasedness, can improve the stability of the convergence process.

In practice, the gradient can be computed as the Monte-Carlo estimate of $\mathbf{g}(\mathbf{u}; \sigma(\phi))$. With $\mathbf{u}_k \sim \prod_{j=1}^p \text{Unif}(0, 1)$, $k = 1, \dots, K$, the Monte-Carlo estimate is

$$\hat{\mathbf{g}}(\phi) = \sum_{k=1}^K \mathbf{g}(\mathbf{u}_k; \sigma(\phi)), \quad (19)$$

where $\mathbf{g}(\cdot)$ is in Eq. (17) or as one of the specific estimators in Eq. (18).

Consider the variance of the gradient estimator $\mathbf{g}(\mathbf{u}; \sigma(\phi))$, *i.e.* the diagonal of the covariance matrix. By the law of total variance, the variance of element v of the gradient vector can be decomposed as

$$\text{var}_{\mathbf{u}}[\mathbf{g}_v(\mathbf{u}; \sigma(\phi))] = \text{var}\{\mathbb{E}[\mathbf{g}_v(\mathbf{u}; \sigma(\phi)) | \mathbf{u}_{-v}]\} + \mathbb{E}\{\text{var}[\mathbf{g}_v(\mathbf{u}; \sigma(\phi)) | \mathbf{u}_{-v}]\}. \quad (20)$$

The first term on the right-hand side (RHS) of Eq. (20) is the irreducible variance, shared by all unbiased gradient estimators. It can be further computed as

$$\text{var}_{\mathbf{u}_{-v}}\{\mathbb{E}_{\mathbf{u}_v}[\mathbf{g}_v(\mathbf{u}; \sigma(\phi)) | \mathbf{u}_{-v}]\} = (\pi_v)^2 (1 - \pi_v)^2 \text{var}_{\mathbf{u}}[\Delta_{\mathbf{z}, v} f],$$

where $\mathbf{z} = \mathbf{1}_{[\mathbf{u} < \sigma(\phi)]}$, $\Delta_{\mathbf{z}, v} f := f(\tilde{\mathbf{z}}) - f(\mathbf{z})$, and $\tilde{\mathbf{z}} \in \{0, 1\}^p$ differing from \mathbf{z} only at the v -th dimension. The second term of Eq. (20) measures the average variance of the estimator vector in a single dimension. Given a fixed \mathbf{u}_{-v} , as shown in the univariate case, U2G estimator has the minimal variance for all estimators in Definition 1 with non-vanishing SNR. Therefore, by averaging over all \mathbf{u}_{-v} , the second term of U2G estimator is small. This means the total variance of U2G estimator is well controlled in the multivariate case.

4 Convergence in Expectation

In this section, we provide theoretical insights to the convergence properties of the gradient method under the expectation of data generation and gradient estimation. We assume that the observations (\mathbf{X}, \mathbf{y}) are generated from the following model with the active set $\mathcal{A} \subset \{1, 2, \dots, p\}$

$$\mathbf{y} = \mathbf{X}\boldsymbol{\beta}^* + \boldsymbol{\epsilon}, \quad \boldsymbol{\epsilon} \sim \mathcal{N}(0, \sigma^2 \mathbf{I}), \quad (21)$$

where $\beta_j^* = 0$ for $j \notin \mathcal{A}$. Let $\mathbf{z}^* \in \{0, 1\}^p$ indicate the true active set where z_j^* equals 1 if $j \in \mathcal{A}$ and 0 otherwise. We assume a random design matrix $\mathbf{X} = (\mathbf{x}_1, \dots, \mathbf{x}_n)^\top$ in which $\mathbf{x}_i \sim \mathcal{N}(0, \mathbf{I}_p)$ for $i \in [n]$. In order to ease the presentation, we denote

$$f_{\mathbf{X}, \mathbf{y}}(\mathbf{z}) = \min_{\boldsymbol{\alpha}} \frac{1}{n} \|\mathbf{y} - \mathbf{X}(\boldsymbol{\alpha} \odot \mathbf{z})\|_2^2 + \lambda \|\mathbf{z}\|_0. \quad (22)$$

Here we use subscripts to make the dependency of f on (\mathbf{X}, \mathbf{y}) explicit. Denote $\mathbf{X}_{\mathbf{z}} \in \mathbb{R}^{n \times \|\mathbf{z}\|_0}$ as the matrix consisting of $\{X_j : z_j \neq 0\}$, and $\mathbf{X}_{-\mathbf{z}}$ the complement in the design matrix. Furthermore, for any $\mathbf{z}, \tilde{\mathbf{z}} \in \{0, 1\}^p$ such that $z_k = 0, \tilde{z}_k = 1, z_j = \tilde{z}_j$ for all $j \neq k$, we denote $\Delta_{\mathbf{z}, k, f} := f_{\mathbf{X}, \mathbf{y}}(\tilde{\mathbf{z}}) - f_{\mathbf{X}, \mathbf{y}}(\mathbf{z})$. All the proof details in this section are given in the appendix.

First, we have the following lemma for the expectation of the gradient over the randomness of \mathbf{u} , given any fixed training data (\mathbf{X}, \mathbf{y}) .

Lemma 1. Consider $g_{\text{U2G}}(\mathbf{u}; \sigma(\phi))$ as in Eq. (18). For each (\mathbf{X}, \mathbf{y}) , we have

$$\mathbb{E}_{\mathbf{u} \sim \prod_{j=1}^p \text{Unif}(u_j; 0, 1)} [g_{\text{U2G}}(\mathbf{u}; \sigma(\phi))] = \boldsymbol{\pi}(1 - \boldsymbol{\pi}) \odot \mathbb{E}_{\mathbf{u}}[\Delta_{\mathbf{z}} f],$$

where $\boldsymbol{\pi} = (\sigma(\phi_1), \dots, \sigma(\phi_p))$, $\mathbf{z} = \mathbf{1}_{[\mathbf{u} > 1 - \sigma(\phi)]}$, and $\Delta_{\mathbf{z}} f = (\Delta_{\mathbf{z}, 1} f, \dots, \Delta_{\mathbf{z}, p} f)$.

Lemma 1 shows that the gradient is closely related to $\Delta_{\mathbf{z}} f$, whose randomness comes from latent variable \mathbf{u} and data (\mathbf{X}, \mathbf{y}) . By analyzing the expectation of $\Delta_{\mathbf{z}} f$, the following result establishes the expectation of stochastic gradients

Lemma 2. Given $g_{\text{U2G}}(\mathbf{u}; \sigma(\phi))$ in Eq. (18), the expected gradient is

$$\begin{aligned} \mathbb{E}_{\mathbf{X}, \mathbf{y}, \mathbf{u}} [g_{\text{U2G}}(\mathbf{u}; \sigma(\phi))_k] &= \left[\lambda - \left(\frac{(n - \mathbb{E}[\|\mathbf{z}\|_0 \mid \|\mathbf{z}\|_0 < n] - 1)(\beta_k^*)^2}{n} \right. \right. \\ &\quad \left. \left. + \frac{\sigma^2 + \mathbb{E}_{\mathbf{u}}[\|\boldsymbol{\beta}_{-\mathbf{z}}^*\|_2^2 \mid \|\mathbf{z}\|_0 < n]}{n} \right) p(\|\mathbf{z}\|_0 < n) \right] \times \pi_k(1 - \pi_k), \end{aligned} \quad (23)$$

for any $k \in \{1, 2, \dots, p\}$ where $\boldsymbol{\pi} = (\sigma(\phi_1), \dots, \sigma(\phi_p))$ and $\mathbf{z} = \mathbf{1}_{[\mathbf{u} > 1 - \sigma(\phi)]}$.

In the following proposition, based on the results of Lemma 2, we show that if the sample size and true coefficient magnitude are not too small, then with proper hyper-parameter λ controlling the penalty strength, each element of the expected gradient points to the direction that can recover the true active set.

Proposition 3. Assume $\sum_{j=1}^p \sigma(\phi_j)/(n-1) \leq 1 - \eta$, for certain $\eta \in (\frac{1}{n}, 1)$. If n is sufficiently large such that $\sqrt{p \log(n)}/2(n-1)^2 \leq \eta$ and $(\|\boldsymbol{\beta}^*\|_2^2 + \sigma^2)/(n-1) \min_{k \in \mathcal{A}} (\beta_k^*)^2 \leq \eta$, then there exists $\lambda > 0$ such that

$$\mathbb{E}_{\mathbf{X}, \mathbf{y}, \mathbf{u}} [g_{\text{U2G}}(\mathbf{u}; \sigma(\phi))_j] < 0, \quad \forall j \in \mathcal{A}; \quad \mathbb{E}_{\mathbf{X}, \mathbf{y}, \mathbf{u}} [g_{\text{U2G}}(\mathbf{u}; \sigma(\phi))_j] > 0, \quad \forall j \notin \mathcal{A}.$$

Remark 1. If the gradient points to the right direction element-wisely, then for each gradient step, in expectation, π_j increases if and only if $j \in \mathcal{A}$. Therefore, if

$$\varpi = \left(1 - \min \left\{ \sqrt{\frac{p \log(n)}{2(n-1)^2}}, \frac{\|\boldsymbol{\beta}^*\|_2^2 + \sigma^2}{(n-1) \min_{k \in \mathcal{A}} (\beta_k^*)^2} \right\} \right) n > S, \quad (24)$$

with initialization

$$\sum_{j=1}^p \pi_j^{(0)} \leq \varpi - S$$

in expectation, $\boldsymbol{\pi}$ in Algorithm 1 converges to the indicator of the true active set.

The proof of Proposition 3 provides a guidance in choosing hyperparameter λ as

$$\lambda \in \left(\frac{\|\boldsymbol{\beta}^*\|_2^2 + \sigma^2}{n}, \frac{n-1}{n} \left(\eta - \frac{1}{n} \right) \min_{j \in \mathcal{A}} (\beta_j^*)^2 \right). \quad (25)$$

Though in practice the true coefficient $\boldsymbol{\beta}^*$ is unknown a priori, choosing $\lambda = \log(n)/(2n)$ as BIC falls in the region (25) asymptotically, and serves as a good initial point for the cross validation in the finite sample case. Now, we study the convergence rate of the updates of Algorithm 1 in expectation, namely, with precise gradient each step. We show that these updates converge to the ground truth after $\mathcal{O}(1/\epsilon)$ steps where $\epsilon > 0$ is the desired accuracy.

Theorem 2. Let the update be $\phi^{(t+1)} = \phi^{(t)} - \rho \mathbb{E}_{\mathbf{x}, \mathbf{y}, \mathbf{u}}[g_{\text{U2G}}(\mathbf{u}; \sigma(\phi^{(t)}))]$ where $\rho > 0$ is the given step size. We assume that $\lambda \in \mathcal{I}$ where \mathcal{I} is defined as in Eq. (25) Furthermore, the initialization $\phi^{(0)}$ satisfies that $\sum_{j=1}^p \sigma(\phi_j^{(0)}) \leq \varpi - S$ where ϖ is defined in Eq. (24). Then, the following holds:

(a) For any $j \in \mathcal{A}$, as long as $t \geq t_j^1$

$$\begin{aligned} \left(1 - \sigma(\phi_j^{(t)})\right) \left[1 - c_1 \sigma^2(\phi_j^{(t)}) \left(1 - \sigma(\phi_j^{(t)})\right)\right] &\leq 1 - \sigma(\phi_j^{(t+1)}) \leq \left(1 - \sigma(\phi_j^{(t)})\right) \\ &\times \left[1 - C_1 (\sigma(\phi_j^{(t)}))^2 \left(1 - \sigma(\phi_j^{(t)})\right)\right]. \end{aligned}$$

(b) For any $j \notin \mathcal{A}$ and $t \geq t_j^2$

$$\begin{aligned} \sigma(\phi_j^{(t)}) \left[1 - c_2 \left(1 - \sigma(\phi_j^{(t)})\right)^2 \sigma(\phi_j^{(t)})\right] &\leq \sigma(\phi_j^{(t+1)}) \leq \sigma(\phi_j^{(t)}) \\ &\times \left[1 - C_2 \left(1 - \sigma(\phi_j^{(t)})\right)^2 \sigma(\phi_j^{(t)})\right]. \end{aligned}$$

Here, with model parameters $\tau = \{n, p, \sigma, \beta^*\}$, c_1, c_2, C_1, C_2 are some positive constants depending only on τ and ρ . t_j^1 and t_j^2 are constants depending on τ, ρ and initial $\phi_j^{(0)}$.

Remark 2. (i) The upper bounds of Theorem 2 demonstrate that when $j \in \mathcal{A}$, $1 - \sigma(\phi_j^{(t)}) \leq \epsilon$ after $t = \mathcal{O}(\epsilon^{-1})$ steps, which is sub-linear. Similarly, when $j \notin \mathcal{A}$, it takes $t = \mathcal{O}(\epsilon^{-1})$ number of iterations for $\sigma(\phi_j^{(t)})$ to be within ϵ radius from 0. The lower bounds in Theorem 2 indicate that these sub-linear complexities are tight. As a consequence, in expectation, the updates of Algorithm 1 converge to the global optima at the sub-linear rate $\mathcal{O}(\epsilon^{-1})$.

(ii) The results of Theorem 2 also yield an insight into the choice of step size ρ . Based on the specific forms of c_1 and c_2 in the proof, we need the step size ρ to satisfy

$$\rho < \min \left\{ \frac{2}{\lambda}, \frac{2}{\max_j \{(\beta_j^*)^2\} - \lambda + (\sigma^2 + \|\beta^*\|_2^2)/n} \right\}. \quad (26)$$

The convergence properties we present in this section are under the expectation. The empirical performance of a low variance gradient estimator such as U2G can be close to the theoretical results, as shown in Section 6. Before that, we extend the proposed gradient methods from solving the frequentist objective (4) to solving the L_0 -regularized regression in the Bayesian paradigm.

5 Bayesian L_0 -Regularized Regression

The objective function in Eq. (5) and the gradient estimators in Section 3 are compatible with a general objective function $f(\mathbf{z})$ with high dimensional binary vector \mathbf{z} . In this section, we consider the best subset selection as a posterior inference problem, and use the gradient estimators in Section 3 to solve the new objective function.

Consider the Bayesian linear regression with the spike-and-slab prior [Mitchell and Beauchamp, 1988, George and McCulloch, 1997], a probabilistic model with the likelihood and prior as

$$\begin{aligned} y_i &\sim \mathcal{N}(\mathbf{x}_i^\top (\boldsymbol{\alpha} \odot \mathbf{z}), \sigma^2), \quad i \in [n] \\ \boldsymbol{\alpha} &\sim \mathcal{N}(\boldsymbol{\alpha}; \mathbf{0}, \boldsymbol{\Sigma}_\alpha), \quad z_j \sim \text{Bern}(\sigma(-\lambda_0)), \quad j \in [p]. \end{aligned} \quad (27)$$

Above, $\boldsymbol{\alpha} \in \mathbb{R}^p$ and $\mathbf{z} \in \{0, 1\}^p$ are latent variables with Gaussian and Bernoulli prior, respectively, and \odot is the element-wise product. The hyper-parameter λ_0 controls the level of sparsity. Setting the regression variable $\boldsymbol{\beta} = \boldsymbol{\alpha} \odot \mathbf{z}$, the prior for $\boldsymbol{\beta}$ is a spike-and-slab prior which has a slab Gaussian component and a spike component at 0,

$$p(\boldsymbol{\beta}) = \prod_{j=1}^p [\sigma(\lambda_0) \delta_0 + (1 - \sigma(\lambda_0)) \mathcal{N}(0, \sigma_\alpha^2)].$$

We consider the *maximum a posterior* (MAP) estimator for the best subset selection. The posterior distribution for the latent variable model in Eq. (27) is

$$p(\boldsymbol{\alpha}, \mathbf{z} \mid \mathbf{X}, \mathbf{y}; \lambda_0, \boldsymbol{\Sigma}_\alpha) \propto \exp \left(- (2\sigma^2)^{-1} \|\mathbf{y} - \mathbf{X}(\boldsymbol{\alpha} \odot \mathbf{z})\|_2^2 - \boldsymbol{\alpha}^\top \boldsymbol{\Sigma}_\alpha^{-1} \boldsymbol{\alpha} / 2 - \lambda_0 \|\mathbf{z}\|_0 \right).$$

Suppose the hyper-parameter $\boldsymbol{\Sigma}_\alpha$ is $\sigma_\alpha^2 \mathbf{I}$. The MAP estimator can be obtained by minimizing the negative log-posterior $-\log p(\boldsymbol{\alpha}, \mathbf{z} \mid \mathbf{X}, \mathbf{y}; \lambda_0, \boldsymbol{\Sigma}_\alpha)$, *i.e.*,

$$\min_{\boldsymbol{\alpha}, \mathbf{z}} \frac{1}{2} \|\mathbf{y} - \mathbf{X}(\boldsymbol{\alpha} \odot \mathbf{z})\|_2^2 + \frac{\sigma^2}{2\sigma_\alpha^2} \|\boldsymbol{\alpha}\|_2^2 + \sigma^2 \lambda_0 \|\mathbf{z}\|_0. \quad (28)$$

By Eq. (28), the MAP estimator of the spike-and-slab regression is equivalent to the solution of the frequentist linear regression with additive L_2 and L_0 penalties [Polson and Sun, 2019]. When the variance σ_α^2 of the slab component in the $\boldsymbol{\beta}$ prior is large, the ratio σ^2/σ_α^2 is small and the MAP estimator of the Bayesian linear regression in Eq. (28) is close to the solution of the best subset selection in Eq. (3).

The MAP estimator is not directly computable because solving Eq. (28) is a combinatorial problem. To overcome the computational challenge, we resort to variational inference (VI) to approximate the posterior distribution and the MAP estimator. To be consistent with VI nomenclature, here we deviate from the notation in Eq. (5), and use $p(\mathbf{z})$ as the prior and $q_\phi(\boldsymbol{\alpha}, \mathbf{z})$ as the variational distribution with parameter ϕ .

The VI methods find an approximated posterior by minimizing the Kullback–Leibler (KL) divergence from $p(\boldsymbol{\alpha}, \mathbf{z} \mid \mathbf{X}, \mathbf{y})$ to $q_\phi(\boldsymbol{\alpha}, \mathbf{z})$, denoted as $D_{\text{KL}}(q_\phi(\boldsymbol{\alpha}, \mathbf{z}) \parallel p(\boldsymbol{\alpha}, \mathbf{z} \mid \mathbf{X}, \mathbf{y}))$. Since the true posterior is often unknown, equivalently we can maximize the evidence lower bound (ELBO) [Blei et al., 2017] as a tractable objective, defined as

$$\begin{aligned} \mathcal{L}(\phi) &= \log p(\mathbf{y} \mid \mathbf{X}) - D_{\text{KL}}(q_\phi(\boldsymbol{\alpha}, \mathbf{z}) \parallel p(\boldsymbol{\alpha}, \mathbf{z} \mid \mathbf{X}, \mathbf{y})) \\ &= \mathbb{E}_{q_\phi(\boldsymbol{\alpha}, \mathbf{z})} \log [p(\mathbf{y} \mid \mathbf{X}, \mathbf{z}, \boldsymbol{\alpha}) p(\boldsymbol{\alpha}, \mathbf{z}; \lambda_0, \sigma_\alpha^2) / q_\phi(\boldsymbol{\alpha}, \mathbf{z})]. \end{aligned} \quad (29)$$

Due to the limited expressiveness of the variational distribution and the zero-forcing property of the KL divergence, variational method often underestimates the posterior uncertainty. Recent analysis, however, provides theoretical guarantees to the accuracy of point estimation. The consistency and asymptotic normality of the VI point estimation have been established for specific models [Bickel et al., 2013, Pati et al., 2018, Zhang and Zhou, 2017, Yin et al., 2020]. A general Bernstein-von Mises theorem has been proved that the variational posterior converges to the KL minimizer of a normal distribution, centered at the truth [Wang and Blei, 2018]. Hence, VI provides an accurate point estimate to the MAP solution, as validated in simulations in Section 6.

To further improve the inference accuracy, we propose a tightened ELBO that is closer to the evidence $\mathcal{L}(\phi)$. By Eq. (29), the gap between ELBO and the evidence equals the KL divergence from the posterior to the variational distribution. We can then reduce the gap by controlling this KL divergence. With the chain rule of the KL divergence,

$$D_{\text{KL}}(q_\phi(\boldsymbol{\alpha}, \mathbf{z}) \parallel p(\boldsymbol{\alpha}, \mathbf{z} \mid \mathbf{X}, \mathbf{y})) = D_{\text{KL}}(q_\phi(\mathbf{z}) \parallel p(\mathbf{z} \mid \mathbf{X}, \mathbf{y})) + \mathbb{E}_{q_\phi(\mathbf{z})} D_{\text{KL}}(q(\boldsymbol{\alpha} \mid \mathbf{z}) \parallel p(\boldsymbol{\alpha} \mid \mathbf{X}, \mathbf{z}, \mathbf{y})). \quad (30)$$

If we choose $q(\boldsymbol{\alpha} \mid \mathbf{z}) = p(\boldsymbol{\alpha} \mid \mathbf{X}, \mathbf{z}, \mathbf{y})$, the second term on the RHS of Eq. (30) becomes 0. Marginalizing out the latent variable $\boldsymbol{\alpha}$, we get a tightened ELBO as

$$\mathcal{L}(\phi) = \mathbb{E}_{q_\phi(\mathbf{z})} \log [p(\mathbf{y} \mid \mathbf{X}, \mathbf{z}; \sigma_\alpha^2) p(\mathbf{z}; \lambda_0) / q_\phi(\mathbf{z})]. \quad (31)$$

To maximize Eq. (31), we choose a mean-field distribution $q_\phi(\mathbf{z}) = \prod_{j=1}^p \text{Bern}(z_j; \sigma(\phi_j))$.

The ELBO in Eq. (31) is a special case of the general optimization objective in Eq. (5) with $f(\mathbf{z}) = \log [p(\mathbf{y} \mid \mathbf{X}, \mathbf{z}; \sigma_\alpha^2) p(\mathbf{z}; \lambda_0) / q_\phi(\mathbf{z})]$. Accordingly, the unbiased gradient estimators in Section 3 can be directly applied to maximizing the ELBO in Eq. (31). The variational objective, compared to the frequentist objective in Eq. (4), does not require computing an OLS solution when evaluating $f(\mathbf{z})$, thus improving efficiency, especially when n is large.

6 Experimental Results

In this section, we study the performance of the gradient-based methods on a variety of synthetic and semi-synthetic data sets. Codes for the simulations in this paper are available at <https://github.com/mingzhang-yin/Probabilistic-Best-Subset>.

Measurement Metrics. Denote $\hat{\beta}$ as the estimated coefficients, β^* as the true coefficients, and (\mathbf{x}, y) as a random sample from the population. We use the population SNR to measure the level of information in data, defined as

$$\text{SNR} := \text{var}(\mathbf{x}^\top \beta^*) / \text{var}(\epsilon) = \beta^{*\top} \Sigma \beta^* / \sigma^2.$$

The population SNR describes the degree of signal in the data generation. In addition to the SNR, the degree of challenge of variable selection is influenced by the number of data n , the number of the covariates p and the size of active set S [Hazimeh and Mazumder, 2018].

The evaluation metrics throughout can be categorized into two groups: one group of metrics measures the out-of-sample predictive performance and the other group measures the recovery quality of the sparsity pattern [Bertsimas et al., 2016, Hastie et al., 2020]. The metrics for the predictive performance that we use are

- *Relative risk (RR)* that measures how model prediction deviates from the oracle prediction, the perfect score being 0:

$$\text{RR}(\hat{\beta}) = \frac{\mathbb{E}(\mathbf{x}^\top \hat{\beta} - \mathbf{x}^\top \beta^*)^2}{\mathbb{E}(\mathbf{x}^\top \beta^*)^2} = \frac{(\hat{\beta} - \beta^*)^\top \Sigma (\hat{\beta} - \beta^*)}{\beta^{*\top} \Sigma \beta^*}.$$

- *Relative test error (RTE)* that measures the relative test MSE compared with the oracle predictor, the perfect score being 1:

$$\text{RTE}(\hat{\beta}) = \frac{\mathbb{E}(y - \mathbf{x}^\top \hat{\beta})^2}{\mathbb{E}(y - \mathbf{x}^\top \beta^*)^2} = \frac{(\hat{\beta} - \beta^*)^\top \Sigma (\hat{\beta} - \beta^*) + \sigma^2}{\sigma^2}.$$

- *Proportion of variance explained (PVE)* that measures the proportion of variance in the response variable explained by the model, the perfect score being $\text{SNR}/(1 + \text{SNR})$:

$$\text{PVE}(\hat{\beta}) = 1 - \frac{\mathbb{E}(y - \mathbf{x}^\top \hat{\beta})^2}{\text{var}(y)} = 1 - \frac{(\hat{\beta} - \beta^*)^\top \Sigma (\hat{\beta} - \beta^*) + \sigma^2}{\beta^{*\top} \Sigma \beta^* + \sigma^2}.$$

To evaluate the sparse pattern recovery, we consider the *size of estimated active set* [Linero, 2018] as well as the *precision*, *recall*, and *F1* scores, given by $\text{prec} = \text{TP}/(\text{TP} + \text{FP})$, $\text{rec} = \text{TP}/(\text{TP} + \text{FN})$, and $\text{F1} = 2 \cdot \text{prec} \cdot \text{rec}/(\text{prec} + \text{rec})$, where TP denotes the number of predictors correctly flagged as influential, FP denotes the number of predictors incorrectly flagged as influential, and FN denotes the number of predictors incorrectly flagged as noninfluential. The F1 score is an overall summary that balances the precision and recall.

Implementation Details. We compare the proposed gradient-based methods with several representative sparse variable selection methods. In particular, we consider LASSO [Tibshirani, 1996], a convex penalty regularized method, SCAD [Fan and Li, 2001], a nonconvex penalty regularized method, and MIO [Bertsimas et al., 2016], Fast-BSS [Hazimeh and Mazumder, 2018], two best subset selection methods.

For the methods in comparison, LASSO is implemented by R package `glmnet` [Friedman et al., 2010]. SCAD is implemented by R package `ncvreg` [Breheny and Huang, 2011]. We use the R package `bestsubset` [Hastie et al., 2018] for the best subset selection with MIO [Bertsimas et al., 2016] and use the R package `LOLearn` [Hazimeh et al., 2022] for the Fast-BSS. The regression functions in `glmnet`, `ncvreg`, `LOLearn` packages fit the regularization hyperparameters over a path of 100 values in default. If not specified, we use the default configurations of the existing R packages.

For the proposed gradient-based methods, we set the number of Monte Carlo samples for estimating the gradient $\mathbb{E}[\mathbf{g}(\mathbf{u}; \sigma(\phi))]$ in Eq. (19) as $K = 20$ throughout the experiments. The gradient-based algorithms take less than 20 seconds to converge when the number of covariates is in thousands, running on a MacBook Pro laptop with a 2.4GHz GHz CPU. To determine the convergence, we compute the entropy for the j -th covariate as $H_j = -\pi_j \log(\pi_j)$ where $\pi_j = \sigma(\phi_j)$ is the probability of the Bernoulli distribution defined in Eq. (3). We stop the training when the average of the 5% largest entropies is below 0.1. Under this stopping criterion, all the probabilities π_j are close to either zero or one. By the analysis in Eq. (4), we choose the hyperparameter λ for the gradient-based methods on a grid of values starting from $\log(n)/(2n)$, and use a constant step-size in SGD smaller than $2/\lambda$.

We choose the hyperparameter for all methods by cross validation. The data is randomly split into training, validation and test sets. We report the results corresponding to the hyperparameter that leads to the lowest prediction error on the validation sets.

Experiment 1: Synthetic Data with Correlated Covariates

We consider the example in Fan and Li [2001] with increased dimension. The true coefficient

$$\boldsymbol{\beta}^* = (3, 1.5, 0, 0, 2, 0, \underbrace{\dots}_{195}, 0) \in \mathbb{R}^{200}.$$

The design matrix \mathbf{X} are n i.i.d. samples generated from $\mathcal{N}(\mathbf{0}, \Sigma)$ where $\Sigma_{ij} = \rho^{|i-j|}$ with the correlation parameter $\rho \in (0, 1)$, and $\mathbf{y} \sim \mathcal{N}(\mathbf{X}\boldsymbol{\beta}^*, \sigma^2\mathbf{I})$. $n = 60$ in this example.

We first compare all the considered methods under a high and a low SNR regime by setting the standard deviation of the noise as $\sigma = 1$ and $\sigma = 3$. As shown in Table 2, the non- L_0 -based methods tend to select larger active sets than the L_0 -regularized regression, reflected as a high recall and a low precision. Furthermore, the best subset methods have lower test error than the non- L_0 -based methods for both SNRs, possibly because the L_0 penalty has no shrinkage effect on the magnitude of the coefficients. For the compared best subset methods, fast-BSS has much higher computational efficiency than MIO due to the cyclic coordinate descent and has better accuracy, which is similarly observed in Hastie et al. [2020]. For the gradient-based methods, U2G and U2G-VI perform on par with or better than ARM₀ and ARM₀-VI, while REINFORCE estimator has a high error in prediction and estimation because of high gradient variance. Based on this observation, we further compare LASSO, SCAD, Fast-BSS, U2G and U2G-VI systematically on a set of extensive experiments.

In Figure 3, we study how the F1 score and relative risk (RR) change with the SNR and the covariate correlation. These metrics reflect the accuracy in estimating the active set and in predicting the outcome of the test data, respectively. We fix the correlation parameter $\rho = 0.5$ and sweep SNR between 1 and 10. Then, we fix SNR = 3 and sweep ρ between 0 and 0.8.

For the active set recovery, we find the L_0 -based methods generally have higher F1 scores than non- L_0 -based methods across all the settings. Among the L_0 -based methods, U2G-VI has the highest F1 score for most SNR and ρ . The F1 score of Fast-BSS drops fast when the covariate correlation ρ increases. In contrast, the gradient-based methods are more robust to high covariate correlation. For the prediction at the test time, we find that when the SNR is below 1.5, non- L_0 -based methods have lower RR than U2G and U2G-VI. We hypothesize that when the SNR is very low, selecting a large set of predictors compensates for the error in the coefficient estimation [Hastie et al., 2020]. A similar phenomenon has been observed that L_0 regularization tends to overfit when the SNR is very low [Mazumder et al., 2017]. For the SNR larger than 1.5 and across different ρ , U2G and U2G-VI have the lowest RR.

We show the regularization path of L_0 regression in Figure 4, with $n = 60, p = 200, \sigma = 1$, and $\rho = 0$. When λ decreases, the number of selected variable increases. The test error first decreases when the correct covariates join the selection, and then increases as additional incorrect covariates are selected. As the top panel shows, for a wide range of λ values, the L_0 -regularized regression recovers the true active set and has an estimated coefficient close to its true value without shrinkage.

Experiment 2: Synthetic Data with Independent Covariates

We consider the experiment in Bertsimas et al. [2016] and Hastie et al. [2020]. The true coefficients have the first 10 elements equal to 1 as $\boldsymbol{\beta}^* = (\underbrace{1, \dots, 1}_{10}, \underbrace{0, \dots, 0}_{990})$ and $p = 1000, S = 10$. The covariates

Table 2: Results of Experiment 1 with $n = 60, p = 200, S = 3$ and $\rho = 0.5$. Reported results are the mean of 100 independent trials.

	Precision	Recall	F1	Nonzero	RR	RTE	PVE
$n = 60, p = 200, \sigma = 1, \text{SNR} = 21.3$							
LASSO	0.780	1.000	0.852	4.65	0.039	1.830	0.918
SCAD	0.983	1.000	0.990	3.07	0.013	1.271	0.943
MIO	1.000	1.000	1.000	3.00	0.003	1.056	0.952
Fast-BSS	1.000	1.000	1.000	3.00	0.003	1.055	0.952
REINFORCE	0.089	0.657	0.153	32.4	1.601	35.01	-
ARM ₀	0.992	1.000	0.996	3.03	0.003	1.067	0.952
U2G	0.990	1.000	0.994	3.04	0.003	1.069	0.952
ARM ₀ (VI)	0.950	1.000	0.971	3.21	0.005	1.107	0.950
U2G(VI)	0.950	1.000	0.971	3.21	0.005	1.107	0.95
$n = 60, p = 200, \sigma = 3, \text{SNR} = 2.4$							
LASSO	0.747	0.850	0.745	4.32	0.284	1.671	0.503
SCAD	0.722	0.777	0.721	3.51	0.214	1.506	0.552
MIO	0.780	0.780	0.780	3.00	0.125	1.294	0.615
Fast-BSS	0.953	0.680	0.787	2.16	0.121	1.292	0.619
REINFORCE	0.092	0.503	0.151	20.2	1.092	3.579	-
ARM ₀	0.856	0.863	0.844	3.15	0.107	1.251	0.628
U2G	0.971	0.850	0.896	2.65	0.063	1.174	0.690
ARM ₀ (VI)	0.921	0.890	0.889	2.96	0.081	1.190	0.646
U2G(VI)	0.913	0.883	0.885	3.00	0.068	1.190	0.686

$\mathbf{x}_i \in \mathbb{R}^{1000}, i \in [n]$ are sampled i.i.d. from a zero mean isotropic Gaussian distribution. SNR = 5 in this example.

Table 3 contains the numerical results for the simulations. LASSO produces a large active set and high RR. SCAD has low prediction error but estimates an excessively large active set. Fast-BSS has high precision and recall but low prediction accuracy. In comparison, U2G and U2G-VI perform well for both target prediction and set estimation.

Table 3: Results of Experiment 2 with $n = 100, p = 1000, S = 10, \text{SNR} = 5$. Reported results are the mean of 100 independent trials.

	Precision	Recall	F1	Nonzero	RR	RTE	PVE
LASSO	0.162	0.995	0.277	63.70	0.259	2.299	0.616
SCAD	0.272	1.000	0.422	39.10	0.050	1.245	0.792
Fast-BSS	0.945	0.940	0.942	9.90	0.109	1.547	0.742
U2G	0.896	0.980	0.934	11.05	0.078	1.391	0.768
U2G(VI)	0.923	1.000	0.950	10.90	0.050	1.256	0.791

Figure 5 explores the influence of the sample size N . For fixed SNR and dimension p , the sample size reflects the level of information contained in the observed data. For small N , the non- L_0 -based methods have a higher F1 score and a lower RR. This indicates that the non- L_0 -based methods are less affected by the scarcity of data, potentially because of the relaxation in the sparsity penalty. When N increases, the best subset methods outperform the non- L_0 -based methods on the F1 score and are on par with SCAD on the RR. In Appendix Figure 9, we study how the number of samples K in estimating the gradient in Eq. (19) influences the performance of U2G and U2G-VI. We find the performance of U2G improves when K increases from 1 to 10 and stays similar when K further increases. The performance of U2G-VI is similar across different values of K .

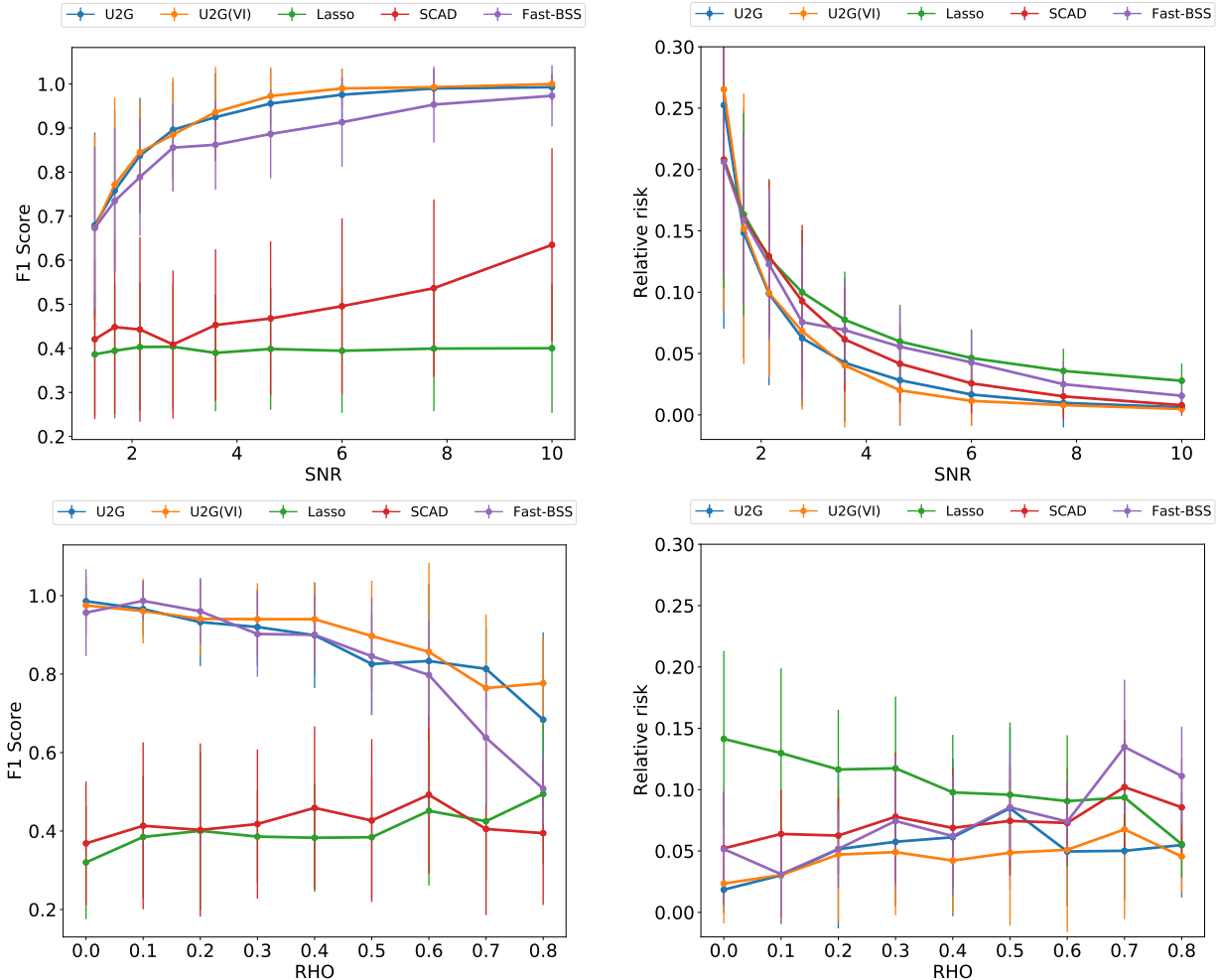


Figure 3: Results for Experiment 1. **Top:** Variable selection across SNR with $\rho = 0.5$. The best subset methods based on L_0 penalty has significantly higher F1 scores in finding the true predictor set. For $\text{SNR} \geq 1.5$, U2G, U2G-VI have the highest F1 scores and the lowest prediction risks. **Bottom:** Variable selection across covariates correlation ρ with $\text{SNR} = 3$. The F1 scores of the best subset methods decrease with an increasing ρ but are higher than that of SCAD and LASSO for all ρ . U2G and U2G-VI have the highest F1 scores in the high correlation regime. U2G-VI has the lowest predictive risk for most of the ρ values.

Experiment 3: Semi-synthetic Data

We further benchmark our methods on Prostate, a real-world microarray dataset about prostate cancer [Singh et al., 2002]. The regularized models are widely used for gene selection as biomarkers in analyzing microarray data, which is often high-dimensional with a large number of genes and a small number of samples. The original Prostate dataset contains the expression profiles of 12,600 genes for 50 normal tissues and 52 prostate tumor tissues. Similar to Bertsimas et al. [2016], we reduce the number of covariates by choosing 1000 genes that maximally correlate (in absolute value) with the tumor type. For the active set, we first choose five gene biomarkers correlated the most with the tumor type, which induces high multi-collinearity in the chosen genes. We also choose five gene biomarkers with pairwise correlation in $(-0.7, 0.7)$ so that the multi-collinearity is moderate. The pairwise correlations are shown in Appendix Figure 8. For each type of active set, we separately create a semi-synthetic data set $\mathbf{y} \sim \mathcal{N}(\mathbf{X}\beta^*, \sigma^2\mathbf{I})$, $\mathbf{X} \in \mathbb{R}^{102 \times 1000}$, where the coefficients are one for the chosen covariates and zero for the other ones.

We compare U2G and U2G-VI with LASSO, SCAD and Fast-BSS, as shown in Table 4 and Appendix Table 7. When the multi-collinearity is moderate in the true active set, the gradient-based method can

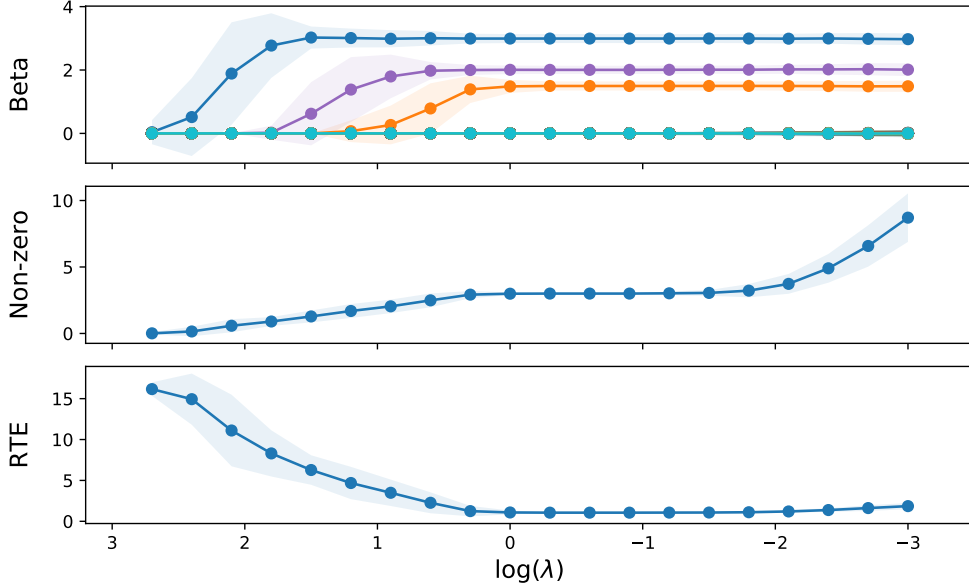


Figure 4: Regularized path for L_0 -regularized regression estimated by U2G gradient, with $n = 60, p = 200, \sigma = 1$. The dotted curves are the mean of 100 independent trials and the shaded areas represent the standard deviation.

Table 4: Results of the Prostate cancer dataset, with $n = 102, p = 1000, S = 5, \text{SNR} = 5$, *moderate* collinearity. Reported results are the average of 100 independent trials.

	Precision	Recall	F1	Nonzero	RR	RTE	PVE
LASSO	0.167	0.980	0.284	31.2	0.049	1.296	0.814
SCAD	0.668	0.940	0.771	7.50	0.020	1.122	0.839
Fast-BSS	0.823	0.900	0.853	5.73	0.037	1.186	0.802
U2G	0.926	0.960	0.942	5.20	0.020	1.12	0.840
U2G(VI)	0.963	0.980	0.971	5.10	0.011	1.067	0.847

recover the true active set with high probability. When the multi-collinearity is high, U2G and U2G-VI have much higher F1 scores and lower RR than the compared methods.

Figure 6 exhibits the performance over a path of SNR from 1 to 10. When the SNR is less than 2, the non- L_0 -based methods have lower RR. When the SNR is moderately large, U2G and U2G-VI have the highest F1 score and U2G-VI has the lowest RR. This is consistent with the observations with the synthetic data in Experiment 1.

Experiment 4: Compressive Sensing

We further study whether the L_0 -based method improves the sparse signal recovery in compressive sensing. The traditional compressive sensing combines the random projection method with L_1 -relaxation [Wainwright, 2019]. It finds the sparse pattern of the observed signal under a set of orthonormal bases while maintaining the exact reconstruction under random projection by a measurement matrix. Following Ji et al. [2008], we consider θ as the coordinates of observations in transformed space with length $p = 1024$, where 10 elements are randomly picked as the signal with magnitude ± 1 . In this example, most of the entries in the true signal are identically zero, which is called *strong sparsity* [Carvalho et al., 2010]. Construing $\mathbf{A} \in \mathbb{R}^{n \times p}$ as a multiplication of the random projection matrix and orthonormal transformation matrix, each row of \mathbf{A} is generated from isotropic Gaussian distribution $\mathcal{N}(0, \mathbf{I}_p)$ and normalized to have the unit norm. We add the Gaussian white noise with a standard deviation σ to the measurements \mathbf{y} . Aligned with our probabilistic

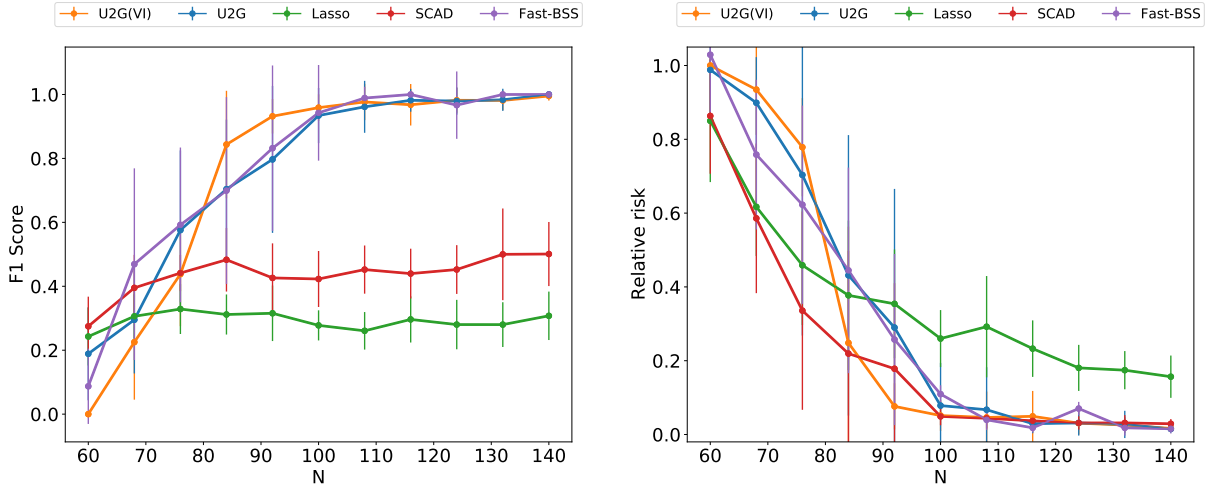


Figure 5: Results for Experiment 2. The change of F1 score and RR with the number of samples with SNR = 5. For a small value of n , non- L_0 -based methods have higher F1 scores and lower RR. For relatively large N the F1 scores of U2G and U2G-VI are close to 1 and xare much higher than those of the non- L_0 -based methods. When $N \geq 100$, the RRs of all compared methods except LASSO are similarly low.

Table 5: Results of the signal reconstruction when SNR_d is low, with $n = 500$, $p = 1000$, $S = 10$, $\sigma = 0.1$. L_0 -based method has the best performance in recovering strong sparsity in the signal.

	Precision	Recall	F1	Nonzero	RR	RTE	PVE
BP	0.009	1.000	0.019	1024	0.298	298	0.702
BCS	0.029	1.000	0.057	336.1	2.380	2381	-
U2G	1.000	1.000	1.000	10.00	0.014	15.1	0.985
U2G(VI)	1.000	1.000	1.000	10.00	0.018	18.6	0.981

objective, we solve the Lagrangian form of

$$\min_{\theta \in \mathbb{R}^p} \|\theta\|_0, \quad \text{such that } \mathbf{A}\theta = \mathbf{y}. \quad (32)$$

We compare U2G with basis pursuit (BP) [Chen et al., 2001] and Bayesian compressive sensing (BCS) [Ji et al., 2008] in different SNR settings by changing the magnitude of σ . For U2G, we use $K = 5$ Monte Carlo samples in the gradient estimation. The numerical results are summarized in Table 5 and Appendix Table 8. As shown in Appendix Figure 10, in the high SNR regime, all three methods can reconstruct the sparse signal reasonably well, but the probabilistic best subset method can identify the locations of true signals, while BP and BCS identify excessively large active sets. Consequently, the L_0 -regularized method has higher predictive precision. This phenomenon is amplified when SNR drops. When SNR is low, as shown in Figure 7, BP and BCS only recover *weak sparsity* where the signals are dense yet most of the entries are small compared to several large ones. In both high and low SNR regimes, the gradient-based methods accurately recover the strong sparsity in the signal, and improve the predictive accuracy of BP and BCS by several orders of magnitude.

7 Discussion

We propose a probabilistic reformulation to solve the exact best subset selection problem using gradient-based optimization. In order to efficiently solve the L_0 -regularized regression in high dimensional settings, a family of unbiased gradient estimators is proposed to approximate the exact gradient. Within this estimator family, we identify the U2G estimator as the one with minimal variance. Theoretically, the U2G estimator recovers

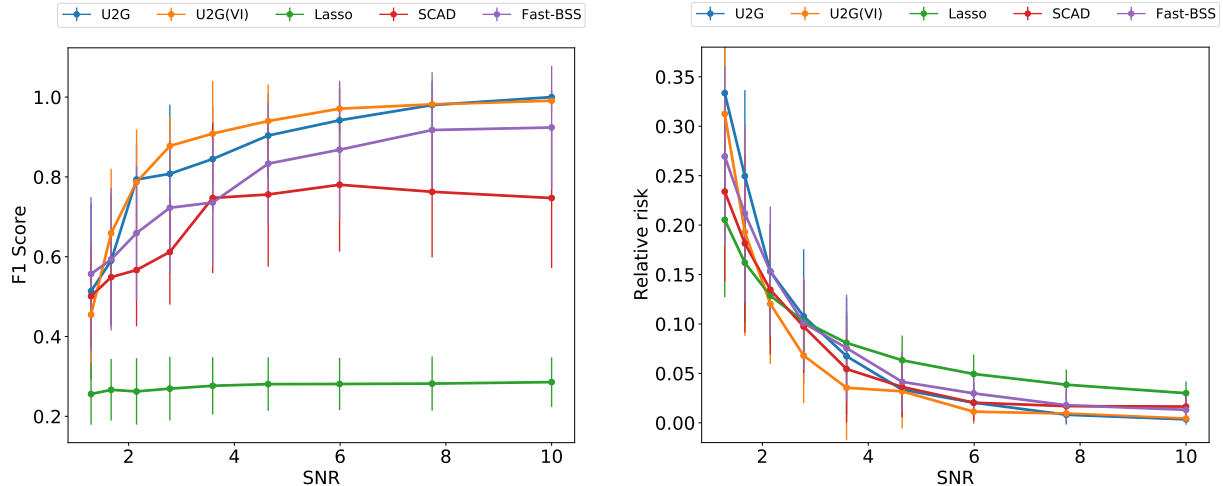


Figure 6: Performance measures on the Prostate cancer data with varying SNR from 1 to 10 with moderate collinearity. U2G-VI has the highest F1 score and the lowest RR when $\text{SNR} \geq 2$.

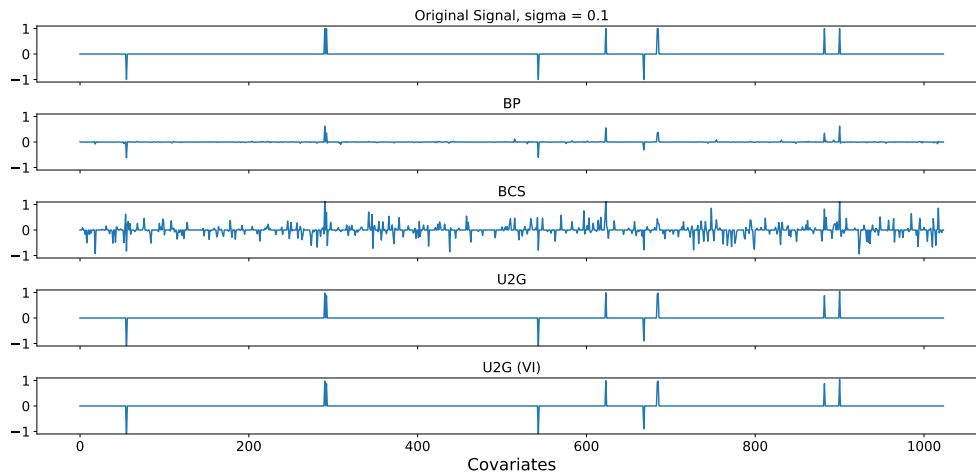


Figure 7: The reconstruction of signals when SNR is low, with $n = 500$, $p = 1024$, $\sigma = 0.1$.

the true sparse pattern in expectation. We also developed a variational method to solve the Bayesian best subset selection with the proposed gradient estimators. Empirically, the proposed gradient-based methods improve the sparsity estimation and predictive accuracy over convex and nonconvex relaxation methods and existing best subset selection tools.

There are several future directions arising naturally. First, the proposed gradient-based methods are highly flexible. A future direction is to analyze the theoretical and empirical properties of the proposed best subset methods on statistical models such as the generalized linear models and deep neural networks. Second, the probabilistic reformulation in this paper is developed for binary variables. An important direction is to generalize it to categorical latent variables [Jang et al., 2017, Tucker et al., 2017, Yin et al., 2019] and find the minimal variance estimator. Third, our theoretical analysis takes a first step with independent covariates and convergence under expectation. Future work is to study the convergence under more general design matrix assumptions. Finally, in this paper, the unbiased gradient estimator is applied in the stochastic gradient descent framework. One future direction is to analyze the update rules with accelerated gradient and momentum [Kingma and Ba, 2014, Ho et al., 2020].

References

- Hirotsugu Akaike. Information theory and an extension of the maximum likelihood principle. In *Selected papers of Hirotsugu Akaike*, pages 199–213. Springer, 1998. [3](#)
- Hirotsugu Akaike. A new look at the statistical model identification. In *Selected Papers of Hirotsugu Akaike*, pages 215–222. Springer, 1974. [3](#)
- Alexandre Belloni and Victor Chernozhukov. Least squares after model selection in high-dimensional sparse models. *Bernoulli*, 19(2):521–547, 2013. [2](#)
- Dimitris Bertsimas, Angela King, and Rahul Mazumder. Best subset selection via a modern optimization lens. *The Annals of Statistics*, 44(2):813–852, 2016. [2](#), [3](#), [13](#), [14](#), [16](#)
- Peter Bickel, David Choi, Xiangyu Chang, and Hai Zhang. Asymptotic normality of maximum likelihood and its variational approximation for stochastic blockmodels. *The Annals of Statistics*, 2013. [12](#)
- David M Blei, Alp Kucukelbir, and Jon D McAuliffe. Variational inference: A review for statisticians. *Journal of the American Statistical Association*, 112(518):859–877, 2017. [12](#)
- Shahin Boluki, Randy Ardywibowo, Siamak Zamani Dadaneh, Mingyuan Zhou, and Xiaoning Qian. Learnable Bernoulli dropout for Bayesian deep learning. In *Artificial Intelligence and Statistics*, 2020. [6](#)
- Patrick Breheny and Jian Huang. Coordinate descent algorithms for nonconvex penalized regression, with applications to biological feature selection. *Annals of Applied Statistics*, 5(1):232–253, 2011. [13](#)
- Emmanuel J Candès and Yaniv Plan. Near-ideal model selection by ℓ_1 minimization. *The Annals of Statistics*, 37(5A):2145–2177, 2009. [2](#)
- Carlos M Carvalho, Nicholas G Polson, and James G Scott. The horseshoe estimator for sparse signals. *Biometrika*, 97(2):465–480, 2010. [17](#)
- Scott Shaobing Chen, David L Donoho, and Michael A Saunders. Atomic decomposition by basis pursuit. *SIAM review*, 43(1):129–159, 2001. [18](#)
- Siamak Zamani Dadaneh, Shahin Boluki, Mingzhang Yin, Mingyuan Zhou, and Xiaoning Qian. Pairwise supervised hashing with Bernoulli variational auto-encoder and self-control gradient estimator. In *Uncertainty in Artificial Intelligence*, 2020. [6](#)
- Lee Dicker, Baosheng Huang, and Xihong Lin. Variable selection and estimation with the seamless- ℓ_0 penalty. *Statistica Sinica*, 23:929–962, 2013. [3](#)
- Zhe Dong, Andriy Mnih, and George Tucker. DisARM: an antithetic gradient estimator for binary latent variables, June 2020. [6](#)
- Jianqing Fan and Runze Li. Variable selection via nonconcave penalized likelihood and its oracle properties. *Journal of the American statistical Association*, 96(456):1348–1360, 2001. [3](#), [13](#), [14](#)
- Jianqing Fan and Jinchi Lv. A selective overview of variable selection in high dimensional feature space. *Statistica Sinica*, 20(1):101, 2010. [1](#), [2](#), [3](#)
- Dean P. Foster and Edward I. George. The risk inflation criterion for multiple regression. *The Annals of Statistics*, 22(4):1947–1975, 1994. [2](#)
- LLdiko E Frank and Jerome H Friedman. A statistical view of some chemometrics regression tools. *Technometrics*, 35(2):109–135, 1993. [2](#)
- Jerome Friedman, Trevor Hastie, and Robert Tibshirani. *The Elements of Statistical Learning*, volume 1. Springer series in statistics New York, 2001. [1](#), [3](#)

- Jerome Friedman, Trevor Hastie, and Rob Tibshirani. Regularization paths for generalized linear models via coordinate descent. *Journal of Statistical Software*, 33(1):1, 2010. [13](#)
- Wenjiang J Fu. Penalized regressions: the bridge versus the lasso. *Journal of Computational and Graphical Statistics*, 7(3):397–416, 1998. [2](#)
- George M Furnival and Robert W Wilson. Regressions by leaps and bounds. *Technometrics*, 16(4):499–511, 1974. [2](#)
- Edward I George and Robert E McCulloch. Variable selection via Gibbs sampling. *Journal of the American Statistical Association*, 88(423):881–889, 1993. [3](#)
- Edward I George and Robert E McCulloch. Approaches for Bayesian variable selection. *Statistica sinica*, pages 339–373, 1997. [11](#)
- Andrés Gómez and Oleg A Prokopyev. A mixed-integer fractional optimization approach to best subset selection. *INFORMS Journal on Computing*, 33(2):551–565, 2021. [2](#)
- Eitan Greenshtein. Best subset selection, persistence in high-dimensional statistical learning and optimization under ℓ_1 constraint. *The Annals of Statistics*, 34(5):2367–2386, 2006. [2](#)
- Evan Greensmith, Peter L Bartlett, and Jonathan Baxter. Variance reduction techniques for gradient estimates in reinforcement learning. *Journal of Machine Learning Research*, 5(9), 2004. [5](#)
- Shixiang Gu, Sergey Levine, Ilya Sutskever, and Andriy Mnih. Muprop: Unbiased backpropagation for stochastic neural networks. *arXiv preprint arXiv:1511.05176*, 2015. [3](#)
- Gurobi Optimization, LLC. Gurobi Optimizer Reference Manual, 2022. URL <https://www.gurobi.com>. [2](#)
- Trevor Hastie, Rob Tibshirani, and Ryan Tibshirani. *Bestsubset: Tools for best subset selection in regression*. R Foundation for Statistical Computing, 2018. R package version 1.0.10. [13](#)
- Trevor Hastie, Robert Tibshirani, and Ryan Tibshirani. Best subset, forward stepwise or lasso? analysis and recommendations based on extensive comparisons. *Statistical Science*, 2020. [2](#), [3](#), [13](#), [14](#)
- Hussein Hazimeh and Rahul Mazumder. Fast best subset selection: Coordinate descent and local combinatorial optimization algorithms, 2018. [2](#), [13](#)
- Hussein Hazimeh, Rahul Mazumder, and Tim Nonet. L0learn: A scalable package for sparse learning using l0 regularization. *arXiv*, 2022. [13](#)
- N. Ho, K. Khamaru, R. Dwivedi, M. J. Wainwright, M. I. Jordan, and B. Yu. Instability, computational efficiency and statistical accuracy. *arXiv preprint arXiv:2005.11411*, 2020. [19](#)
- Eric Jang, Shixiang Gu, and Ben Poole. Categorical reparameterization with Gumbel-softmax. In *5th International Conference on Learning Representations, ICLR 2017, Toulon, France, April 24-26, 2017, Conference Track Proceedings*. OpenReview.net, 2017. [3](#), [5](#), [19](#)
- Shihao Ji, Ya Xue, and Lawrence Carin. Bayesian compressive sensing. *IEEE Transactions on signal processing*, 56(6):2346, 2008. [17](#), [18](#)
- Kory D Johnson, Dongyu Lin, Lyle H Ungar, Dean P Foster, and Robert A Stine. A risk ratio comparison of ℓ_0 and ℓ_1 penalized regression, 2015. [2](#)
- Diederik P Kingma and Jimmy Ba. Adam: A method for stochastic optimization. *arXiv preprint arXiv:1412.6980*, 2014. [19](#)
- Antonio R Linero. Bayesian regression trees for high-dimensional prediction and variable selection. *Journal of the American Statistical Association*, 113(522):626–636, 2018. [13](#)
- Yufeng Liu and Yichao Wu. Variable selection via a combination of the ℓ_0 and ℓ_1 penalties. *Journal of Computational and Graphical Statistics*, 16(4):782–798, 2007. [3](#)

- Chris J Maddison, Andriy Mnih, and Yee Whye Teh. The concrete distribution: A continuous relaxation of discrete random variables. In *ICLR*, 2016. [3](#)
- Rahul Mazumder, Peter Radchenko, and Antoine Dedieu. Subset selection with shrinkage: Sparse linear modeling when the snr is low. *arXiv preprint arXiv:1708.03288*, 2017. [14](#)
- Toby J Mitchell and John J Beauchamp. Bayesian variable selection in linear regression. *Journal of the american statistical association*, 83(404):1023–1032, 1988. [2](#), [11](#)
- Shakir Mohamed, Mihaela Rosca, Michael Figurnov, and Andriy Mnih. Monte carlo gradient estimation in machine learning. *J. Mach. Learn. Res.*, 21(132):1–62, 2020. [3](#)
- Balas Kausik Natarajan. Sparse approximate solutions to linear systems. *SIAM Journal on Computing*, 24(2):227–234, 1995. [2](#)
- Debdeep Pati, Anirban Bhattacharya, and Yun Yang. On statistical optimality of variational Bayes. In *International Conference on Artificial Intelligence and Statistics*, pages 1579–1588, 2018. [12](#)
- Jan Peters and Stefan Schaal. Policy gradient methods for robotics. In *2006 IEEE/RSJ International Conference on Intelligent Robots and Systems*, pages 2219–2225. IEEE, 2006. [5](#)
- Nicholas G Polson and Lei Sun. Bayesian l 0-regularized least squares. *Applied Stochastic Models in Business and Industry*, 35(3):717–731, 2019. [12](#)
- Sheldon M Ross. *Introduction to probability models*. Academic press, 2014. [8](#)
- Gideon Schwarz. Estimating the dimension of a model. *The Annals of Statistics*, 6(2):461–464, 1978. [3](#)
- Robert J Serfling. *Approximation theorems of mathematical statistics*. John Wiley & Sons, 2009. [4](#)
- Xiaotong Shen, Wei Pan, and Yunzhang Zhu. Likelihood-based selection and sharp parameter estimation. *Journal of the American Statistical Association*, 107(497):223–232, 2012. [3](#)
- Dinesh Singh, Phillip G Febbo, Kenneth Ross, Donald G Jackson, Judith Manola, Christine Ladd, Pablo Tamayo, Andrew A Renshaw, Anthony V D’Amico, Jerome P Richie, et al. Gene expression correlates of clinical prostate cancer behavior. *Cancer cell*, 1(2):203–209, 2002. [16](#)
- T Tao. Singularity and determinant of random matrices. Technical report, Lewis Memorial Lecture, 2008. [24](#)
- Robert Tibshirani. Regression shrinkage and selection via the lasso. *Journal of the Royal Statistical Society: Series B (Methodological)*, 58(1):267–288, 1996. [13](#)
- George Tucker, Andriy Mnih, Chris J Maddison, John Lawson, and Jascha Sohl-Dickstein. Rebar: Low-variance, unbiased gradient estimates for discrete latent variable models. In *Advances in Neural Information Processing Systems*, pages 2627–2636, 2017. [3](#), [5](#), [19](#)
- Martin J Wainwright. Sharp thresholds for high-dimensional and noisy sparsity recovery using ℓ_1 -constrained quadratic programming (lasso). *IEEE Transactions on Information Theory*, 2009. [2](#)
- Martin J Wainwright. *High-dimensional statistics: A non-asymptotic viewpoint*, volume 48. Cambridge University Press, 2019. [17](#)
- Yixin Wang and David M Blei. Frequentist consistency of variational Bayes. *Journal of the American Statistical Association*, 114(527):1147–1161, 2018. [12](#)
- Ronald J Williams. Simple statistical gradient-following algorithms for connectionist reinforcement learning. In *Reinforcement Learning*, pages 5–32. Springer, 1992. [4](#)
- Yutaro Yamada, Ofir Lindenbaum, Sahand Negahban, and Yuval Kluger. Feature selection using stochastic gates. In *International Conference on Machine Learning*, pages 10648–10659. PMLR, 2020. [3](#)

- Mingzhang Yin and Mingyuan Zhou. ARM: Augment-REINFORCE-merge gradient for stochastic binary networks. In *International Conference on Learning Representations*, 2019. [3](#), [5](#)
- Mingzhang Yin, Yuguang Yue, and Mingyuan Zhou. ARSM: Augment-reinforce-swap-merge estimator for gradient backpropagation through categorical variables. In *International Conference on Machine Learning*, pages 7095–7104, 2019. [19](#)
- Mingzhang Yin, YX Wang, and Purnamrita Sarkar. A theoretical case study of structured variational inference for community detection. In *International Conference on Artificial Intelligence and Statistics*, 2020. [12](#)
- Yuguang Yue, Yunhao Tang, Mingzhang Yin, and Mingyuan Zhou. Discrete action on-policy learning with action-value critic. In *Artificial Intelligence and Statistics*, 2020. [3](#), [6](#)
- Anderson Y Zhang and Harrison H Zhou. Theoretical and computational guarantees of mean field variational inference for community detection, 2017. [12](#)
- Cun-Hui Zhang. Nearly unbiased variable selection under minimax concave penalty. *The Annals of Statistics*, 38(2):894–942, 2010. [3](#)
- Cun-Hui Zhang and Tong Zhang. A general theory of concave regularization for high-dimensional sparse estimation problems. *Statistical Science*, 27(4):576–593, 2012. [2](#)
- Peng Zhao and Bin Yu. On model selection consistency of lasso. *Journal of Machine learning research*, 7 (Nov):2541–2563, 2006. [2](#)

Supplementary Material for “Probabilistic Best Subset Selection via Gradient-Based Optimization”

This supplementary document contains detailed proofs and derivations of the theoretical results presented in the main paper, and additional experimental results. In particular, Appendix A contains a necessary lemma for the proof of convergence properties. Appendix B contains proofs of the theoretical results presented in the main paper. Finally, Appendix C contains additional simulation results on the semi-synthetic data and compressive sensing.

A Auxiliary Lemmas

The following lemma describes the linear independence between random Gaussian vectors, which is useful when the sample size exceeds the number of covariates. Closely following the proof in Tao [2008], which contains a thorough discussion on the singularity of random matrix ensembles, we have the following result:

Lemma 3. *Let $X_j \in \mathbb{R}^n$ are i.i.d. random Gaussian vectors with distribution $\mathcal{N}(0, \mathbf{I}_n)$, for $j = 1, \dots, k$, $k \leq n$. Then $\{X_1, \dots, X_k\}$ are linearly independent with probability one.*

Proof. Let event \mathcal{E} be the event that $\{X_1, \dots, X_k\}$ are linearly dependent. Then \mathcal{E} is equivalent to that X_j lies in the span of X_1, \dots, X_{j-1} for some j . Thus

$$p(\mathcal{E}) \leq \sum_{j=2}^k p(X_j \in V_j),$$

where $V_j := \text{span}(X_1, \dots, X_{j-1})$. For each $2 \leq j \leq k$, conditional on vectors X_1, \dots, X_{j-1} , the vector space V_j is fixed, has positive codimension, and thus has measure zero. Since the distribution of X_j is absolutely continuous, and is independent of X_1, \dots, X_{j-1} , we have

$$p(X_j \in V_j | X_1, \dots, X_{j-1}) = 0$$

for all (X_1, \dots, X_{j-1}) . Integrating over (X_1, \dots, X_{j-1}) , we have $p(X_j \in V_j) = 0$; therefore

$$p(\mathcal{E}) \leq \sum_{j=2}^k p(X_j \in V_j) = 0,$$

which proves that $\{X_1, \dots, X_k\}$ are linearly independent with probability 1. As a consequence, we obtain the conclusion of the lemma. Q.E.D.

B Proofs

In this appendix, we provide proofs for theoretical results in the paper.

B.1 Proof of Theorem 1

Proof. On the one hand, we show the optimal solution to problem (3) is in the set of feasible solutions to problem (4). Assuming (α^*, \mathbf{z}^*) is the optimal solution to problem (3), setting $p_j = z_j^*$, $j \in [p]$ and $\alpha = \alpha^*$ would be a feasible solution to problem (4) which gives the same object value as what (α^*, \mathbf{z}^*) achieves in problem (3).

On the other hand, we show the optimal solution to problem (4) is in the set of feasible solutions to problem (3). Let $h(\mathbf{z}) = \frac{1}{n} \|\mathbf{y} - \mathbf{X}(\alpha \odot \mathbf{z})\|^2 + \lambda \|\mathbf{z}\|_0$, $f(\mathbf{z}) = \min_{\alpha} h(\mathbf{z})$, $g(\mathbf{z}) = \arg \min_{\alpha} h(\mathbf{z})$, and assume π^* is the optimal π in problem (4). First, if $p(\mathbf{z} | \pi^*)$ is a point mass density $\delta_{\mathbf{z}^*}$ with $\pi_j^* = z_j^*$, $j \in [p]$ and $\alpha^* = g(\mathbf{z}^*)$, by setting $\mathbf{z} = \pi^*$, $\alpha = \alpha^*$, it would give a feasible solution to problem (3) with the same objective value as problem (4). Second, if $p(\mathbf{z} | \pi^*)$ is not a point mass density, assume $\text{supp}[p(\mathbf{z} | \pi^*)] = \{\mathbf{z}_1, \dots, \mathbf{z}_K\}$. We show

by contradiction that all the points in $\text{supp}[p(\mathbf{z}|\boldsymbol{\pi}^*)]$ would give the same objective value $f(\mathbf{z})$. Otherwise there exist $\mathbf{z}_s, \mathbf{z}_l \in \text{supp}[p(\mathbf{z}|\boldsymbol{\pi}^*)]$ with $f(\mathbf{z}_s) < f(\mathbf{z}_l)$ and $f(\mathbf{z}_s) \leq f(\mathbf{z}_k)$ for $k \neq s, l$. By setting $\hat{\pi}_j = z_{ij}$, we would have $\mathbb{E}_{\mathbf{z} \sim p(\mathbf{z}|\hat{\boldsymbol{\pi}})} f(\mathbf{z}) < \mathbb{E}_{\mathbf{z} \sim p(\mathbf{z}|\boldsymbol{\pi}^*)} f(\mathbf{z})$ which contradicts with the assumption that $\boldsymbol{\pi}^*$ is optimal. Therefore, we have $f(\mathbf{z}_1) = f(\mathbf{z}_2) = \dots = f(\mathbf{z}_K)$. Hence all points in $\{\mathbf{z}_k, g(\mathbf{z}_k)\}_{k \in [K]}$ are feasible solutions to problem (3) which give the same objective value as what the optimal solution gives in problem (4).

In summary, we show problem (3) and (4) have the same global optima and the same objective value at such points, so they are equivalent problems. Q.E.D.

B.2 Proof of Proposition 1

Proof. Without loss of generality, we assume that $f(1), f(0) > 0$, $\pi = \sigma(\phi) \geq 1/2$, and let $\Delta = f(1) - f(0)$. For the first inequality, direct calculation shows that

$$\begin{aligned} \text{var}[g_{\text{ARM}}] - \text{var}[g_R] &= \mathbb{E}_u[g_{\text{ARM}}^2] - \mathbb{E}_u[g_R^2] \\ &= s_1 f(1)^2 + s_2 f(0)^2 + s_3 f(1)f(0) \\ &= (s_1 + s_2 + s_3) f(0)^2 + s_1 \Delta^2 + (2s_1 + s_3) f(0) \Delta \\ &\leq (s_1 + s_2 + s_3) f(0)^2 + (3s_1 + s_3) f(0)^2 \end{aligned}$$

where $s_1 = -\frac{5}{3}\pi^3 + 3\pi^2 - \frac{3}{2}\pi + \frac{1}{6}$, $s_2 = \frac{1}{3}\pi^3 - \frac{1}{2}\pi + \frac{1}{6}$, $s_3 = \frac{4}{3}\pi^3 - 2\pi^2 + \pi - \frac{1}{3}$. Re-organizing the coefficients, we have

$$\text{var}[g_{\text{ARM}}] - \text{var}[g_R] \leq -\left[\pi\left(1 - \frac{\pi}{6}\right) + \frac{21\pi + 1}{6}(1 - \pi)\right] f(0)^2 \leq 0.$$

For the second inequality, we find that

$$\text{var}[g_{\text{U2G}}] - \text{var}[g_{\text{ARM}}] = \mathbb{E}_u[g_{\text{U2G}}^2] - \mathbb{E}_u[g_{\text{ARM}}^2] = -\frac{(1 - \pi)^3}{6} (f(1) - f(0))^2 \leq 0.$$

As a consequence, we obtain the conclusion of the proposition. Q.E.D.

B.3 Proof of Proposition 2

Proof. We consider a constrained optimization problem

$$\min_g \int_0^1 g^2(u) du, \quad \text{subject to } \mathbb{E}[g(u)] = \mu,$$

where $\mu = \pi(1 - \pi)(f_1 - f_0)$. For simplicity, we omit the conditional notation on π if it is clear. The integration can be decomposed into three intervals $[0, 1 - \pi]$, $(1 - \pi, \pi]$, $(\pi, 1]$, so we can rewrite Eq. (9) into a piece-wise function.

$$g(u) = \begin{cases} g_1(u) := a(u)f_1 + b(u)f_0, & u \in [0, 1 - \pi] \\ g_2(u) := a(u)f_1 + b(u)f_1, & u \in (1 - \pi, \pi] \\ g_3(u) := a(u)f_0 + b(u)f_1, & u \in (\pi, 1] \end{cases}$$

And we would like to minimize

$$\mathbb{E}[g^2(u)] = \mathbb{E}_{u \in [0, 1 - \pi]}[g_1^2(u)] + \mathbb{E}_{u \in [1 - \pi, \pi]}[g_2^2(u)] + \mathbb{E}_{u \in [\pi, 1]}[g_3^2(u)].$$

If there exists π and a positive measure subset $\mathcal{S}_\pi \subset (1 - \pi, \pi]$ where $|a(u; \pi) + b(u; \pi)| \geq \epsilon_\pi > 0$ and $f_1 \neq 0$, then

$$\mathbb{E}[g^2(u; \pi)] \geq \mathbb{E}[g_2^2(u; \pi)] \geq \epsilon_\pi^2 |\mathcal{S}_\pi| f_1^2.$$

This means that

$$\lim_{\Delta \rightarrow 0} \text{var}[g(u; \pi)] = \lim_{\Delta \rightarrow 0} \mathbb{E}[g^2(u; \pi)] - \mu^2$$

$$= \lim_{\Delta \rightarrow 0} \mathbb{E}[g^2(u; \pi)] \geq \epsilon_\pi^2 |\mathcal{S}_\pi| f_1^2 > 0,$$

which contradicts the condition (14). Therefore if the estimator has positive SNR for $\pi \in (0, 1)$, it has to satisfy $a(u) + b(u) = 0$ almost surely (a.s.) in $(1 - \pi, \pi]$ or has $f_1 = 0$, where in both cases $g(u) = 0$ a.s. for $u \in (1 - \pi, \pi]$. Assume $g(u) = 0$ for $u \in (1 - \pi, \pi]$ a.s., we have

$$\begin{aligned} \text{var}[g(u; \pi)] &= (1 - \pi) \left[\int_0^{1-\pi} \frac{1}{1 - \pi} g^2(u) du + \int_\pi^1 \frac{1}{1 - \pi} g^2(u) du \right] - \mu^2 \\ &\geq \frac{1}{1 - \pi} \left\{ \left[\int_0^{1-\pi} g(u) du \right]^2 + \left[\int_\pi^1 g(u) du \right]^2 \right\} - \mu^2 \\ &= \frac{1}{1 - \pi} (2s^2 - 2\mu s + \mu^2) - \mu^2 \\ &\geq \frac{2\pi - 1}{2(1 - \pi)} \mu^2, \end{aligned}$$

where $s = \int_0^{1-\pi} g(u) du$; both inequalities are equalities if and only if $g(u) = \frac{\mu}{2(1-\pi)}$ for $u \in [0, 1 - \pi] \cup (\pi, 1]$. Together with the premise $g(u) = 0$ for $u \in (1 - \pi, \pi]$ a.s., we get the U2G estimator. The same argument holds for $\pi < 0.5$ because of the symmetry. Q.E.D.

B.4 Proof of Lemma 1

Proof. In order to ease the presentation, we denote $\mathbf{z} = \mathbf{1}_{[u > 1 - \sigma(\phi)]}$, $\tilde{\mathbf{z}} = \mathbf{1}_{[u < \sigma(\phi)]}$, $\pi_j = \sigma(\phi_j) \forall j \in \{1, \dots, p\}$. Then we have $\mathbf{g}_{\text{U2G}}(\mathbf{u}; \sigma(\phi)) = \frac{f(\mathbf{z}) - f(\tilde{\mathbf{z}})}{2} \sigma(|\phi|) \odot (\mathbf{1}_{[u > 1 - \sigma(\phi)]} - \mathbf{1}_{[u < \sigma(\phi)]})$. Construct a sequence of binary code $\mathbf{z}^0 = \mathbf{z}, \mathbf{z}^1, \dots, \mathbf{z}^p = \tilde{\mathbf{z}}$ by flipping one dimension of \mathbf{z} to the value in $\tilde{\mathbf{z}}$ at a time, i.e., $\mathbf{z}^i = (\tilde{z}_1, \dots, \tilde{z}_i, z_{i+1}, \dots, z_p)'$. Hence $f_{\mathbf{X}, \mathbf{y}}(\mathbf{z}) - f_{\mathbf{X}, \mathbf{y}}(\tilde{\mathbf{z}}) = \sum_{i=1}^p (f_{\mathbf{X}, \mathbf{y}}(\mathbf{z}^{i-1}) - f_{\mathbf{X}, \mathbf{y}}(\mathbf{z}^i))$. We prove the statement for the gradient vector element-wisely. Consider the j^{th} dimension of the gradient vector

$$\mathbb{E}_{\mathbf{u}} [g(\mathbf{u})_j] = \frac{\sigma(|\phi_j|)}{2} \mathbb{E}_{\mathbf{u}} \sum_{i=1}^p (f_{\mathbf{X}, \mathbf{y}}(\mathbf{z}^{i-1}) - f_{\mathbf{X}, \mathbf{y}}(\mathbf{z}^i)) (\mathbf{1}_{[u_j > \sigma(-\phi_j)]} - \mathbf{1}_{[u_j < \sigma(\phi_j)]}) \quad (33)$$

Note that \mathbf{z}^{i-1} and \mathbf{z}^i only differ on the i^{th} dimension, and different dimensions of \mathbf{u} are independent. Consider the i^{th} element of the summation in Eq.(33) and W.L.O.G. we first assume the logit $\phi_i \geq 0$. For $i \neq j$, due to the symmetry of the sigmoid function, we have

$$\begin{aligned} &\mathbb{E}_{\mathbf{u}} \frac{\sigma(|\phi_j|)}{2} (f_{\mathbf{X}, \mathbf{y}}(\mathbf{z}^{i-1}) - f_{\mathbf{X}, \mathbf{y}}(\mathbf{z}^i)) (\mathbf{1}_{[u_j > \sigma(-\phi_j)]} - \mathbf{1}_{[u_j < \sigma(\phi_j)]}) \\ &= \frac{\sigma(|\phi_j|)}{2} \mathbb{E}_{\mathbf{u}_{-i}} [\mathbb{E}_{u_i} [f_{\mathbf{X}, \mathbf{y}}(\mathbf{z}^{i-1}) - f_{\mathbf{X}, \mathbf{y}}(\mathbf{z}^i)] (\mathbf{1}_{[u_j > \sigma(-\phi_j)]} - \mathbf{1}_{[u_j < \sigma(\phi_j)]}) | \mathbf{u}_{-i}] \\ &= \frac{\sigma(|\phi_j|)}{2} \mathbb{E}_{\mathbf{u}_{-i}} [(\mathbf{1}_{[u_j > \sigma(-\phi_j)]} - \mathbf{1}_{[u_j < \sigma(\phi_j)]}) \mathbb{E}_{u_i} [f_{\mathbf{X}, \mathbf{y}}(\mathbf{z}^{i-1}) - f_{\mathbf{X}, \mathbf{y}}(\mathbf{z}^i)] | \mathbf{u}_{-i}] \\ &= \mathbb{E}_{\mathbf{u}_{-i}} [(\mathbf{1}_{[u_j > \sigma(-\phi_j)]} - \mathbf{1}_{[u_j < \sigma(\phi_j)]}) \left(\int_0^{\sigma(-\phi_i)} (f_{\mathbf{X}, \mathbf{y}}(\mathbf{z}^{i-1} | z_i = 0) - f_{\mathbf{X}, \mathbf{y}}(\mathbf{z}^i | z_i = 1)) du_i \right. \\ &\quad \left. + \int_{\sigma(\phi_i)}^1 (f_{\mathbf{X}, \mathbf{y}}(\mathbf{z}^{i-1} | z_i = 1) - f_{\mathbf{X}, \mathbf{y}}(\mathbf{z}^i | z_i = 0)) du_i \right) | \mathbf{u}_{-i}] \frac{\sigma(|\phi_j|)}{2} \\ &= \mathbb{E}_{\mathbf{u}_{-i}} [(\mathbf{1}_{[u_j > \sigma(-\phi_j)]} - \mathbf{1}_{[u_j < \sigma(\phi_j)]}) \left((f_{\mathbf{X}, \mathbf{y}}(\mathbf{z}^{i-1} | z_i = 0) - f_{\mathbf{X}, \mathbf{y}}(\mathbf{z}^i | z_i = 1)) (1 - \sigma(\phi_i)) \right. \\ &\quad \left. + (f_{\mathbf{X}, \mathbf{y}}(\mathbf{z}^{i-1} | z_i = 1) - f_{\mathbf{X}, \mathbf{y}}(\mathbf{z}^i | z_i = 0)) (1 - \sigma(\phi_i)) \right) | \mathbf{u}_{-i}] \frac{\sigma(|\phi_j|)}{2} \\ &= 0. \end{aligned}$$

Whereas for $i = j$, we have

$$\frac{\sigma(|\phi_j|)}{2} \mathbb{E}_{\mathbf{u}} (f_{\mathbf{X}, \mathbf{y}}(\mathbf{z}^{j-1}) - f_{\mathbf{X}, \mathbf{y}}(\mathbf{z}^j)) (\mathbf{1}_{[u_j > \sigma(-\phi_j)]} - \mathbf{1}_{[u_j < \sigma(\phi_j)]})$$

$$\begin{aligned}
&= \frac{\sigma(\phi_j)}{2} \mathbb{E}_{\mathbf{u}_{-j}} \left[\mathbb{E}_{u_j} [(f_{\mathbf{X}, \mathbf{y}}(\mathbf{z}^{j-1}) - f_{\mathbf{X}, \mathbf{y}}(\mathbf{z}^j))(\mathbf{1}_{[u_j > \sigma(-\phi_j)]} - \mathbf{1}_{[u_j < \sigma(\phi_j)]}) | \mathbf{u}_{-j}] \right] \\
&= \frac{\sigma(\phi_j)}{2} \mathbb{E}_{\mathbf{u}_{-j}} \left[\left(\int_0^{\sigma(-\phi_j)} (f_{\mathbf{X}, \mathbf{y}}(\mathbf{z}^{j-1} | z_j = 0) - f_{\mathbf{X}, \mathbf{y}}(\mathbf{z}^j | z_j = 1)) (-1) du_j \right. \right. \\
&\quad \left. \left. + \int_{\sigma(\phi_j)}^1 (f_{\mathbf{X}, \mathbf{y}}(\mathbf{z}^{j-1} | z_j = 1) - f_{\mathbf{X}, \mathbf{y}}(\mathbf{z}^j | z_j = 0)) du_j \right) \middle| \mathbf{u}_{-j} \right] \\
&= \mathbb{E}_{\mathbf{u}_{-j}} \left[\sigma(\phi_j)(1 - \sigma(\phi_j)) [f_{\mathbf{X}, \mathbf{y}}(\mathbf{z}^{j-1} | z_j = 1) - f_{\mathbf{X}, \mathbf{y}}(\mathbf{z}^j | z_j = 0)] \right] \\
&= \pi_j(1 - \pi_j) \mathbb{E}_{\mathbf{u}} [\Delta_{z,j} f].
\end{aligned}$$

The same derivation holds true when the logit $\phi_i \leq 0$. Hence for each dimension there is only one non-zero element in the summation of Eq.(33). Rewriting the result in vector form proves the lemma. Q.E.D.

B.5 Proof of Lemma 2

Proof. Based on Lemma 1, it suffices to compute the expectation of $\mathbb{E}_{\mathbf{X}, \mathbf{y}, \mathbf{u}} [\Delta_{z} f]$ to obtain the conclusion of Lemma 2, where $\Delta_{z} f = (\Delta_{z,1} f, \dots, \Delta_{z,p} f)$. For any $k \in [p]$, direct application of conditional expectation formulations leads to

$$\begin{aligned}
\mathbb{E}_{\mathbf{X}, \mathbf{y}, \mathbf{u}} [\Delta_{z,k} f] &= \mathbb{E} [\Delta_{z,k} f | \|\mathbf{z}\|_0 < n-1] p(\|\mathbf{z}\|_0 < n-1) \\
&\quad + \mathbb{E} [\Delta_{z,k} f | \|\mathbf{z}\|_0 = n-1] p(\|\mathbf{z}\|_0 = n-1) + \mathbb{E} [\Delta_{z,k} f | \|\mathbf{z}\|_0 \geq n] p(\|\mathbf{z}\|_0 \geq n).
\end{aligned} \tag{34}$$

Conditioned on the event $\|\mathbf{z}\|_0 < n-1$, we denote projection matrix $P_{\mathbf{z}} = \mathbf{X}_{\mathbf{z}} (\mathbf{X}_{\mathbf{z}}^{\top} \mathbf{X}_{\mathbf{z}})^{-1} \mathbf{X}_{\mathbf{z}}^{\top}$ for any \mathbf{z} and the OLS estimator $\hat{\alpha}_{\mathbf{z}} = (\mathbf{X}_{\mathbf{z}}^{\top} \mathbf{X}_{\mathbf{z}})^{-1} \mathbf{X}_{\mathbf{z}}^{\top} \mathbf{y}$. Under that event, given the definition of $\Delta_{z,k} f$ we obtain that

$$\begin{aligned}
\Delta_{z,k} f &= \lambda + \frac{1}{n} \|\mathbf{y} - \mathbf{X}_{\tilde{\mathbf{z}}} \hat{\alpha}_{\tilde{\mathbf{z}}}\|_2^2 - \frac{1}{n} \|\mathbf{y} - \mathbf{X}_{\mathbf{z}} \hat{\alpha}_{\mathbf{z}}\|_2^2 \\
&= \lambda + \underbrace{\frac{1}{n} \|\mathbf{y} - \mathbf{X}_{\tilde{\mathbf{z}}} \hat{\alpha}_{\tilde{\mathbf{z}}}\|_2^2 - \frac{1}{n} \|\mathbf{y} - \mathbf{X}_{\tilde{\mathbf{z}}} \beta_{\tilde{\mathbf{z}}}^*\|_2^2}_{:=T_1} \\
&\quad + \underbrace{\frac{1}{n} \|\mathbf{y} - \mathbf{X}_{\tilde{\mathbf{z}}} \beta_{\tilde{\mathbf{z}}}^*\|_2^2 - \frac{1}{n} \|\mathbf{y} - \mathbf{X}_{\mathbf{z}} \beta_{\mathbf{z}}^*\|_2^2}_{:=T_2} + \underbrace{\frac{1}{n} \|\mathbf{y} - \mathbf{X}_{\mathbf{z}} \beta_{\mathbf{z}}^*\|_2^2 - \frac{1}{n} \|\mathbf{y} - \mathbf{X}_{\mathbf{z}} \hat{\alpha}_{\mathbf{z}}\|_2^2}_{:=T_3},
\end{aligned} \tag{35}$$

where $\tilde{\mathbf{z}} \in \{0, 1\}^p$ is such that \mathbf{z} and $\tilde{\mathbf{z}}$ only differ on dimension k , i.e., $z_k = 0, \tilde{z}_k = 1, z_j = \tilde{z}_j, \forall j \neq k$. Note that, $\|\tilde{\mathbf{z}}\|_0 = \|\mathbf{z}\|_0 + 1 \leq n-1$ when $\|\mathbf{z}\|_0 < n-1$; therefore, the OLS estimator $\hat{\alpha}_{\tilde{\mathbf{z}}} = (\mathbf{X}_{\tilde{\mathbf{z}}}^{\top} \mathbf{X}_{\tilde{\mathbf{z}}})^{-1} \mathbf{X}_{\tilde{\mathbf{z}}}^{\top} \mathbf{y}$ is valid. Regarding term T_1 in equation (35), direct computation shows that

$$T_1 = -\frac{1}{n} (\mathbf{X}_{-\tilde{\mathbf{z}}} \beta_{-\tilde{\mathbf{z}}}^* + \epsilon)^{\top} P_{\tilde{\mathbf{z}}} (\mathbf{X}_{-\tilde{\mathbf{z}}} \beta_{-\tilde{\mathbf{z}}}^* + \epsilon) = -\frac{1}{n} \|P_{\tilde{\mathbf{z}}} (\mathbf{X}_{-\tilde{\mathbf{z}}} \beta_{-\tilde{\mathbf{z}}}^* + \epsilon)\|_2^2. \tag{36}$$

By Lemma 3, conditioned on \mathbf{u} , the rank of $X_{\tilde{\mathbf{z}}}$ equals $\|\tilde{\mathbf{z}}\|_0$ with probability one. Taking the expectation of T_1 with respect to \mathbf{X}, \mathbf{y} , a key observation is that for any $X_{\tilde{\mathbf{z}}}$ with full column rank,

$$\mathbb{E}_{\mathbf{X}, \mathbf{y}} [T_1 | X_{\tilde{\mathbf{z}}}, \|\mathbf{z}\|_0 < n-1] = -\frac{(\sigma^2 + \|\beta_{-\tilde{\mathbf{z}}}^*\|_2^2) \|\tilde{\mathbf{z}}\|_0}{n}. \tag{37}$$

Therefore, we obtain that

$$\mathbb{E}_{\mathbf{X}, \mathbf{y}} [T_1 | \|\mathbf{z}\|_0 < n-1] = \mathbb{E}_{\mathbf{X}, \mathbf{y}} [\mathbb{E} [T_1 | X_{\tilde{\mathbf{z}}}, \|\mathbf{z}\|_0 < n-1]] = -\frac{(\sigma^2 + \|\beta_{-\tilde{\mathbf{z}}}^*\|_2^2) \|\tilde{\mathbf{z}}\|_0}{n}. \tag{38}$$

The above result leads to

$$\mathbb{E}_{\mathbf{X}, \mathbf{y}, \mathbf{u}} [T_1 | \|\mathbf{z}\|_0 < n-1] = -\mathbb{E}_{\mathbf{u}} \left[\frac{(\sigma^2 + \|\beta_{-\tilde{\mathbf{z}}}^*\|_2^2) \|\tilde{\mathbf{z}}\|_0}{n} \middle| \|\mathbf{z}\|_0 < n-1 \right].$$

For the term T_3 in equation (35), similar argument proves that

$$\mathbb{E}_{\mathbf{X}, \mathbf{y}, \mathbf{u}}[T_3 \mid \|\mathbf{z}\|_0 < n-1] = \mathbb{E}_{\mathbf{u}} \left[\frac{(\sigma^2 + \|\boldsymbol{\beta}_{-\mathbf{z}}^*\|_2^2) \|\mathbf{z}\|_0}{n} \mid \|\mathbf{z}\|_0 < n-1 \right].$$

For the term T_2 in equation (35), direct calculation shows that

$$T_2 = -(\beta_k^*)^2 \frac{1}{n} \|X_k\|^2 - \frac{2}{n} \beta_k^* X_k^\top R_{\tilde{\mathbf{z}}},$$

where $R_{\tilde{\mathbf{z}}} = \mathbf{X}_{-\tilde{\mathbf{z}}} \boldsymbol{\beta}_{-\tilde{\mathbf{z}}}^* + \boldsymbol{\epsilon}$. Therefore, $\mathbb{E}_{\mathbf{X}, \mathbf{y}, \mathbf{u}}[T_2 \mid \|\mathbf{z}\|_0 < n-1] = -(\beta_k^*)^2$.

Putting the above results together, we find that

$$\begin{aligned} \mathbb{E}_{\mathbf{X}, \mathbf{y}, \mathbf{u}}[\Delta_{z,k} f \mid \|\mathbf{z}\|_0 < n-1] &= \lambda - \frac{1}{n} \left((\beta_k^*)^2 (n - \mathbb{E}_{\mathbf{u}}[\|\mathbf{z}\|_0 \mid \|\mathbf{z}\|_0 < n-1]) - 1 \right) \\ &\quad + \sigma^2 + \mathbb{E}_{\mathbf{u}}[\|\boldsymbol{\beta}_{-\mathbf{z}}^*\|_2^2 \mid \|\mathbf{z}\|_0 < n-1]. \end{aligned} \quad (39)$$

Conditioned on the event $\|\mathbf{z}\|_0 = n-1$, recall that

$$\Delta_{z,k} f = \lambda - \frac{1}{n} \|\mathbf{y} - \mathbf{X}_{\mathbf{z}} \hat{\boldsymbol{\alpha}}_{\mathbf{z}}\|_2^2 = \lambda - \frac{1}{n} \|(I_n - P_z) W_{\mathbf{z}}\|_2^2,$$

where $W_{\mathbf{z}} = \mathbf{X}_{-\mathbf{z}} \boldsymbol{\beta}_{-\mathbf{z}}^* + \boldsymbol{\epsilon}$. Conditioned on \mathbf{u} , $W_{\mathbf{z}} \sim \mathcal{N}(0, (\sigma^2 + \|\boldsymbol{\beta}_{-\mathbf{z}}^*\|_2^2) I_n)$. Therefore, we obtain that

$$\mathbb{E}_{\mathbf{X}, \mathbf{y}} \left[\frac{1}{n} \|(I_n - P_z) W_{\mathbf{z}}\|_2^2 \mid \|\mathbf{z}\|_0 = n-1 \right] = \frac{\sigma^2 + \|\boldsymbol{\beta}_{-\mathbf{z}}^*\|_2^2}{n}.$$

The above inequality shows that

$$\mathbb{E}_{\mathbf{X}, \mathbf{y}, \mathbf{u}}[\Delta_{z,k} f \mid \|\mathbf{z}\|_0 = n-1] = \lambda - \frac{\sigma^2 + \mathbb{E}_{\mathbf{u}}[\|\boldsymbol{\beta}_{-\mathbf{z}}^*\|_2^2 \mid \|\mathbf{z}\|_0 = n-1]}{n}. \quad (40)$$

Finally, we compute $\mathbb{E}_{\mathbf{X}, \mathbf{y}, \mathbf{u}}[\Delta_{z,k} f \mid \|\mathbf{z}\|_0 \geq n]$. Under the setting $\|\mathbf{z}\|_0 \geq n$, we have $\|\tilde{\mathbf{z}}\|_0 \geq n+1$. By Lemma 3, conditioned on \mathbf{u} , with probability one, we have $\min_{\boldsymbol{\alpha}} \frac{1}{n} \|\mathbf{y} - \mathbf{X}_{\mathbf{z}} \boldsymbol{\alpha}\|_2^2 = 0$ and $\min_{\boldsymbol{\alpha}} \frac{1}{n} \|\mathbf{y} - \mathbf{X}_{\tilde{\mathbf{z}}} \boldsymbol{\alpha}\|_2^2 = 0$. Therefore, conditioned on \mathbf{u} and $\|\mathbf{z}\|_0 \geq n$, with probability one, we obtain that

$$\Delta_{z,k} f = \lambda.$$

It directly leads to

$$\mathbb{E}_{\mathbf{X}, \mathbf{y}, \mathbf{u}}[\Delta_{z,k} f \mid \|\mathbf{z}\|_0 \geq n] = \lambda. \quad (41)$$

Plugging the results of equations (39), (40), and (41) into the equation (34), we obtain the conclusion of the lemma. Q.E.D.

B.6 Proof of Proposition 3

Proof. We consider cases whether the covariates are in the true active set separately.

Case 1 - $\{j : \beta_j^* = 0\}$: when $\|\mathbf{z}\|_0 < n$, by Lemma 2, we have

$$\begin{aligned} \mathbb{E}_{\mathbf{X}, \mathbf{y}, \mathbf{u}}[g_{UG}(\mathbf{u}; \sigma(\phi))_j] &= \left(\lambda - \frac{\sigma^2 + \mathbb{E}_{\mathbf{u}}[\|\boldsymbol{\beta}_{-\mathbf{z}}^*\|_2^2 \mid \|\mathbf{z}\|_0 < n]}{n} \right) \pi_j (1 - \pi_j) \\ &\geq \left(\lambda - \frac{\sigma^2 + \|\boldsymbol{\beta}^*\|_2^2}{n} \right) \pi_j (1 - \pi_j), \end{aligned}$$

where the inequality is due to $\|\beta_{-z}^*\|_2^2 \leq \|\beta^*\|_2^2$ for all z . Therefore, if $\lambda > (\sigma^2 + \|\beta^*\|_2^2)/n$, we have $\mathbb{E}_{\mathbf{x}, \mathbf{y}, \mathbf{u}}[g_{U2G}(\mathbf{u}; \sigma(\phi))_j] > 0$ for all $j \notin \mathcal{A}$.

Case 2 - $\{j : \beta_j^* \neq 0\}$: by Hoeffding's inequality for sub-Gaussian random variables, and by the assumption $p \leq 2\eta^2(n-1)^2/\log(n)$, we have

$$p(\|\mathbf{z}\|_0 \geq n-1) \leq \exp\left(-\frac{2(n-1 - \sum_{k=1}^p \pi_j)^2}{p}\right) \leq \frac{1}{n}.$$

Furthermore, simple algebra shows that

$$\mathbb{E}\left[\|\mathbf{z}\|_0 \mid \|\mathbf{z}\|_0 < n-1\right] \leq \mathbb{E}[\|\mathbf{z}\|_0] = \sum_{k=1}^p \pi_k.$$

Collecting the previous results and using the result of Lemma 2, we find that

$$\begin{aligned} \mathbb{E}_{\mathbf{x}, \mathbf{y}, \mathbf{u}}[g_{U2G}(\mathbf{u}; \sigma(\phi))_j] &\leq \left(\lambda - \frac{(\beta_j^*)^2(n-1)}{n}\left(1 - \frac{1}{n}\right) + \frac{(\beta_j^*)^2(\sum_{k=1}^p \pi_k)}{n}\right) \pi_j(1 - \pi_j) \\ &\leq \left(\lambda - (\beta_j^*)^2 \left[\frac{(n-1)^2}{n^2} - \frac{\sum_{k=1}^p \pi_k}{n}\right]\right) \pi_j(1 - \pi_j) \\ &\leq \left(\lambda - (\beta_j^*)^2 \frac{n-1}{n} \left(\eta - \frac{1}{n}\right)\right) \pi_j(1 - \pi_j). \end{aligned} \quad (42)$$

Therefore, as long as $\lambda < \frac{n-1}{n}(\eta - \frac{1}{n}) \min_{k \in \mathcal{A}} (\beta_k^*)^2$, we have $\mathbb{E}_{\mathbf{x}, \mathbf{y}, \mathbf{u}}[g_{U2G}(\mathbf{u}; \sigma(\phi))_j] < 0$ for all $j \in \mathcal{A}$. Combining the two cases, by setting

$$\lambda \in \left(\frac{\|\beta^*\|_2^2 + \sigma^2}{n}, \frac{n-1}{n} \left(\eta - \frac{1}{n}\right) \min_{k \in \mathcal{A}} (\beta_k^*)^2\right) := \mathcal{I}, \quad (43)$$

the proposition is proved. Q.E.D.

B.7 Proof of Theorem 2

Proof. For the simplicity of the presentation, we denote

$$G(\phi) := \mathbb{E}_{\mathbf{x}, \mathbf{y}, \mathbf{u}}[g_{U2G}(\mathbf{u}; \sigma(\phi))]/[\boldsymbol{\pi}(1 - \boldsymbol{\pi})],$$

where $\boldsymbol{\pi} = \sigma(\phi)$ and the division is element-wise. Furthermore, we denote

$$\eta = \min \left\{ \sqrt{\frac{p \log(n)}{2(n-1)^2}}, \frac{\|\beta^*\|_2^2 + \sigma^2}{(n-1) \min_{k \in \mathcal{A}} (\beta_k^*)^2} \right\}.$$

We now state our proof with two parts.

(a) Since $\lambda \in \mathcal{I}$ and $\sum_{j=1}^p \sigma(\phi_j^{(0)}) \leq \varpi - S$, we have $G(\phi_j^{(t)}) < 0$ for all $j \in \mathcal{A}$. It shows that the updates $\phi_j^{(t+1)}$ are monotonically increasing, i.e., $\phi_j^{(t+1)} > \phi_j^{(t)}$ for any $t \geq 0$ and $j \in \mathcal{A}$. For any $t \geq 0$, we obtain that

$$\phi_j^{(t+1)} = \phi_j^{(0)} - \rho \left(\sum_{i=0}^t \mathbb{E}_{\mathbf{x}, \mathbf{y}, \mathbf{u}}[g_{U2G}(\mathbf{u}; \sigma(\phi^{(i)}))_j] \right).$$

We now study the lower bound of t such that $\phi_j^{(t+1)} \geq 0$ for the first time. In order to study that, we assume that $\phi_j^{(i)} < 0$ for all $0 \leq i \leq t$. Based on the proof of Proposition 3, for any $0 \leq i \leq t$, we have

$$\mathbb{E}_{\mathbf{x}, \mathbf{y}, \mathbf{u}}[g_{U2G}(\mathbf{u}; \sigma(\phi^{(i)}))_j] \leq \left(\lambda - (\beta_j^*)^2 \frac{n-1}{n} \left(\eta - \frac{1}{n}\right)\right) \sigma(\phi_j^{(i)})(1 - \sigma(\phi_j^{(i)}))$$

$$\leq \left(\lambda - (\beta_j^*)^2 \frac{n-1}{n} \left(\eta - \frac{1}{n} \right) \right) \sigma(\phi_j^{(0)}) (1 - \sigma(\phi_j^{(0)})),$$

where the second inequality is due to the fact that $\sigma_j^{(0)} \leq \sigma_j^{(i)} < 0$ for all $0 \leq i \leq t$. Collecting the above results, we find that

$$\phi_j^{(t+1)} \geq \phi_j^{(0)} - \rho t \left(\lambda - (\beta_j^*)^2 \frac{n-1}{n} \left(\eta - \frac{1}{n} \right) \right) \sigma(\phi_j^{(0)}) (1 - \sigma(\phi_j^{(0)})).$$

Therefore, as long as $t \geq \frac{\phi_j^{(0)}}{\rho \left(\lambda - (\beta_j^*)^2 \frac{n-1}{n} \left(\eta - \frac{1}{n} \right) \right) \sigma(\phi_j^{(0)}) (1 - \sigma(\phi_j^{(0)}))} := T_1$, we have $\phi_j^{(t+1)} \geq 0$.

By using the inequality $\sigma(x+y) \leq \sigma(x) + y\sigma'(x)$ for any $x, y > 0$, for any $j \in \mathcal{A}$ and $t \geq T_1$ we obtain that

$$\begin{aligned} 1 - \sigma(\phi_j^{(t+1)}) &\geq 1 - \sigma(\phi_j^{(t)}) + \rho G(\phi_j^{(t)}) \sigma(\phi_j^{(t)}) (1 - \sigma(\phi_j^{(t)})) \sigma'(\phi_j^{(t)}) \\ &= \left(1 - \sigma(\phi_j^{(t)}) \right) \left[1 + \rho \sigma^2(\phi_j^{(t)}) G(\phi_j^{(t)}) \left(1 - \sigma(\phi_j^{(t)}) \right) \right]. \end{aligned} \quad (44)$$

Based on the result of Lemma 2, we find that

$$G(\phi_j^{(t)}) \geq \lambda - \frac{\sigma^2 + \|\beta^*\|_2^2 + (n-1)(\beta_i^*)^2}{n}, \quad (45)$$

which is due to $\|\beta_{-z}^*\|_2^2 \leq \|\beta^*\|_2^2$ and $\|z\|_0 \geq 0$ for all z . Plugging this inequality into equation (44), we achieve the conclusion of the lower bound in part (a) with $c_1 = \rho[(\sigma^2 + \|\beta^*\|_2^2 + (n-1)(\beta_i^*)^2)/n - \lambda] > 0$.

Regarding the upper bound, we first prove that

$$\sigma(x+y) \geq \sigma(x) + \exp(-y)y\sigma'(x) \quad (46)$$

for all $x, y > 0$. In fact, from the mean-value theorem, there exists $\xi \in (x, x+y)$ such that $\sigma'(\xi) = (\sigma(x+y) - \sigma(x))/y$. Since the function $\sigma'(\cdot)$ is monotonically decreasing in $(0, \infty)$, we have $\sigma'(\xi) \geq \sigma'(x+y)$. Simple calculation yields that $\sigma'(x+y)/\sigma'(x) \geq \exp(-y)$ for all $x, y > 0$. Therefore, we obtain the conclusion of inequality (46). Given the inequality (46), for any $t \geq T_1$ we have

$$\begin{aligned} 1 - \sigma(\phi_j^{(t+1)}) &\leq 1 - \sigma(\phi_j^{(t)}) \\ &\quad + \exp\left(\rho\sigma(\phi_j^{(t)})(1 - \sigma(\phi_j^{(t)}))G(\phi_j^{(t)})\right) \rho G(\phi_j^{(t)}) \sigma^2(\phi_j^{(t)}) (1 - \sigma(\phi_j^{(t)}))^2. \end{aligned} \quad (47)$$

Since $G(\phi_j^{(t)}) < 0$ and $\phi_j^{(t)} \geq 0$, an application of the bound (45) and standard inequality $\sigma(\phi_j^{(t)})(1 - \sigma(\phi_j^{(t)})) \leq 1/4$ leads to

$$\sigma(\phi_j^{(t)})(1 - \sigma(\phi_j^{(t)}))G(\phi_j^{(t)}) \geq \frac{1}{4} \left(\lambda - \frac{\sigma^2 + \|\beta^*\|_2^2 + (n-1)(\beta_i^*)^2}{n} \right). \quad (48)$$

Furthermore, using the proof argument of Proposition 3, we find that

$$G(\phi_j^{(t)}) \leq \lambda - (\beta_i^*)^2 \frac{n-1}{n} \left(\eta - \frac{1}{n} \right), \quad (49)$$

where $\eta = \min \left\{ \sqrt{p \log(n)/2n^2}, (\|\beta^*\|_2^2 + \sigma^2)/(n-1) \min_{k \in \mathcal{A}} (\beta_k^*)^2 \right\}$. Plugging the bounds (48) and (49) into the equation (47), we obtain the conclusion of the upper bound in part (a) with C_1 is given by

$$C_1 = \rho \exp \left(\frac{\rho}{4} \left(\lambda - \frac{\sigma^2 + \|\beta^*\|_2^2 + (n-1)(\beta_i^*)^2}{n} \right) \right) \left((\beta_i^*)^2 \frac{n-1}{n} \left(\eta - \frac{1}{n} \right) - \lambda \right) > 0.$$

As a consequence, we obtain the conclusion of the upper bound in part (a).

(b) The proof of part (b) follows the same line of proof argument as that in part (a). Indeed, since $\lambda \in \mathcal{I}$ and $\sum_{j=1}^p \sigma(\phi_j^{(0)}) \leq \varpi - S$, we have $G(\phi_j^{(t)}) > 0$ for all $j \notin \mathcal{A}$. It shows that the updates $\phi_j^{(t+1)}$ are monotonically decreasing, *i.e.*, $\phi_j^{(t+1)} < \phi_j^{(t)}$ for any $t \geq 0$ and $j \notin \mathcal{A}$. Similar to part (a), we first find a lower bound on t such that $\phi_j^{(t+1)} \leq 0$. In fact, we assume that $\phi_j^{(i)} > 0$ for all $0 \leq i \leq t$. Then, based on the proof of Proposition 3, for any $0 \leq i \leq t$, we find that

$$\begin{aligned} \mathbb{E}_{\mathbf{X}, \mathbf{y}, \mathbf{u}}[g_{U2G}(\mathbf{u}; \sigma(\phi^{(i)}))_j] &\geq \left(\lambda - \frac{\sigma^2 + \|\boldsymbol{\beta}^*\|_2^2}{n} \right) \sigma(\phi_j^{(i)})(1 - \sigma(\phi_j^{(i)})) \\ &\geq \left(\lambda - \frac{\sigma^2 + \|\boldsymbol{\beta}^*\|_2^2}{n} \right) \sigma(\phi_j^{(0)})(1 - \sigma(\phi_j^{(0)})), \end{aligned}$$

where the second inequality is due to the fact that $\sigma_j^{(0)} \geq \sigma_j^{(i)} > 0$ for any $0 \leq i \leq t$. Therefore, we obtain that

$$\phi_j^{(t+1)} \leq \phi_j^{(0)} - \rho t \left(\lambda - \frac{\sigma^2 + \|\boldsymbol{\beta}^*\|_2^2}{n} \right) \sigma(\phi_j^{(0)})(1 - \sigma(\phi_j^{(0)})).$$

The above inequality demonstrates that as long as $t \geq \frac{\phi_j^{(0)}}{\rho \left(\lambda - \frac{\sigma^2 + \|\boldsymbol{\beta}^*\|_2^2}{n} \right) \sigma(\phi_j^{(0)})(1 - \sigma(\phi_j^{(0)}))} := T_2$, we have

$$\phi_j^{(t+1)} \leq 0.$$

Now, we can check that $\sigma(x - y) \geq \sigma(x) - y\sigma'(x)$ for all $x < 0$ and $y > 0$. Using this inequality, for any $j \notin \mathcal{A}$ and $t \geq T_2$ we obtain that

$$\sigma(\phi_j^{(t+1)}) \geq \sigma(\phi_j^{(t)}) - \rho G(\phi_j^{(t)}) \sigma(\phi_j^{(t)})(1 - \sigma(\phi_j^{(t)})) \sigma'(\phi_j^{(t)}).$$

From the result of Lemma 2, it is clear that $G(\phi_j^{(t)}) \leq \lambda$ for all $j \notin \mathcal{A}$. Therefore, we have

$$\sigma(\phi_j^{(t+1)}) \geq \sigma(\phi_j^{(t)}) \left[1 - \lambda \rho (1 - \sigma(\phi_j^{(t)}))^2 \sigma(\phi_j^{(t)}) \right].$$

We achieve the conclusion of the lower bound in part (b) with $c_2 = \rho\lambda > 0$.

Moving to the upper bound, with similar argument as that of equation (46), we can check that

$$\sigma(x - y) \geq \sigma(x) - \exp(-y)y\sigma'(x),$$

for any $x < 0$ and $y > 0$. Given that inequality, for any $t \geq T_2$ we obtain that

$$\begin{aligned} \sigma(\phi_j^{(t+1)}) &\leq \sigma(\phi_j^{(t)}) \\ &\quad - \exp\left(-\rho\sigma(\phi_j^{(t)})(1 - \sigma(\phi_j^{(t)}))G(\phi_j^{(t)})\right) \rho G(\phi_j^{(t)}) \sigma(\phi_j^{(t)})(1 - \sigma(\phi_j^{(t)})) \sigma'(\phi_j^{(t)}). \end{aligned} \quad (50)$$

Based on the result of Lemma 2, we can check that $\sigma(\phi_j^{(t)})(1 - \sigma(\phi_j^{(t)}))G(\phi_j^{(t)}) \leq \lambda/4$ and $G(\phi_j^{(t)}) \geq \lambda - (\sigma^2 + \|\boldsymbol{\beta}^*\|_2^2)/n$. Putting the above results together, we have

$$\sigma(\phi_j^{(t+1)}) \leq \sigma(\phi_j^{(t)}) \left[1 - C_2 (1 - \sigma(\phi_j^{(t)}))^2 \sigma(\phi_j^{(t)}) \right],$$

for any $t \geq T_2$ where $C_2 = \rho \exp(-\rho\lambda/4) \left(\lambda - (\sigma^2 + \|\boldsymbol{\beta}^*\|_2^2)/n \right) > 0$. As a consequence, we reach the conclusion of the upper bound in part (b). Q.E.D.

C Additional Results

In this appendix, we provide additional experimental results. For the Prostate cancer dataset, Figure 8 shows the pairwise correlations of the two types of chosen covariates in the true active set. Table 7 summarizes the results for the variable selection methods when the multi-collinearity in the true active set is high.

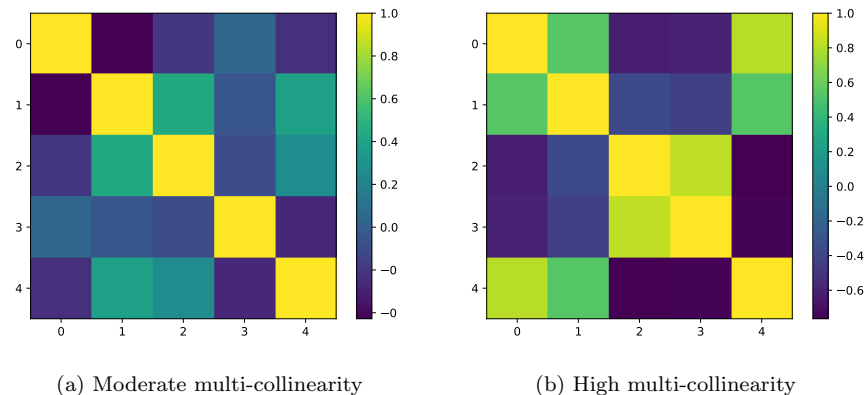


Figure 8: Two types of correlations between the covariates in the true active sets, Prostate cancer dataset.

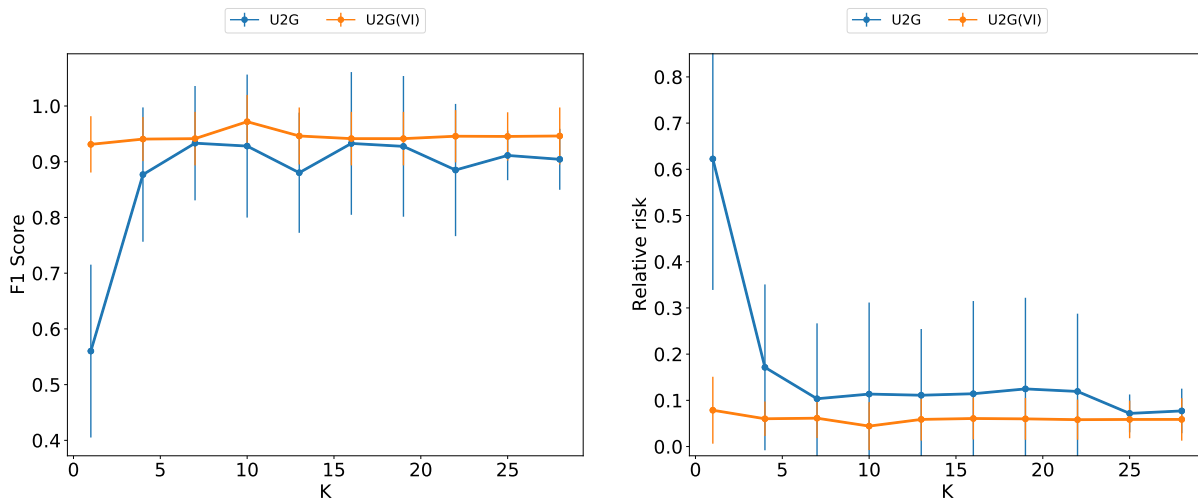


Figure 9: The F1 score and RR of U2G and U2G-VI over different number of samples K in estimating the gradient. U2G performance increases with K when K is small and U2G-VI has similar performance across different K .

For the compressive sensing, as shown in Figure 10 and Table 8, when SNR is high, all methods can achieve low prediction error but BP and BCS cannot set the coefficients of the non-signal covariates as exact zero. As shown in Figure 7, when SNR is low, methods with L_1 penalty cannot recover strong sparsity, but our method with L_0 penalty can.

Table 6: Results of the variable selection simulation study, with $n = 100$, $p = 1000$, $S = 10$, $\text{SNR} = 5$. Reported results are the mean of 100 independent trials.

	Precision	Recall	F1	Nonzero	RR	RTE	PVE
LASSO	0.162	0.995	0.277	63.70	0.259	2.299	0.616
SCAD	0.272	1.000	0.422	39.10	0.050	1.245	0.792
MIO	0.674	0.674	0.674	10.00	0.444	3.220	0.463
Fast-BSS	0.945	0.940	0.942	9.90	0.109	1.547	0.742
REINFORCE	0.011	0.497	0.021	471.6	1.085	6.426	-
ARM ₀	0.906	0.906	0.904	10.01	0.154	1.771	0.705
U2G	0.896	0.980	0.934	11.05	0.078	1.391	0.768
ARM ₀ (VI)	0.954	0.967	0.960	10.13	0.075	1.374	0.771
U2G(VI)	0.923	1.000	0.950	10.90	0.050	1.256	0.791

Table 7: Results of the Prostate cancer dataset, with $n = 102$, $p = 1000$, $S = 5$, *high* multi-collinearity. Reported results are the average of 100 independent trials.

	Precision	Recall	F1	Nonzero	RR	RTE	PVE
LASSO	0.091	0.712	0.160	44.9	0.090	1.454	0.759
SCAD	0.270	0.368	0.306	7.04	0.427	3.144	0.478
Fast-BSS	0.336	0.302	0.312	4.58	0.194	1.982	0.672
U2G	0.852	0.796	0.818	4.73	0.058	1.292	0.785
U2G(VI)	0.936	0.812	0.863	4.34	0.057	1.286	0.786

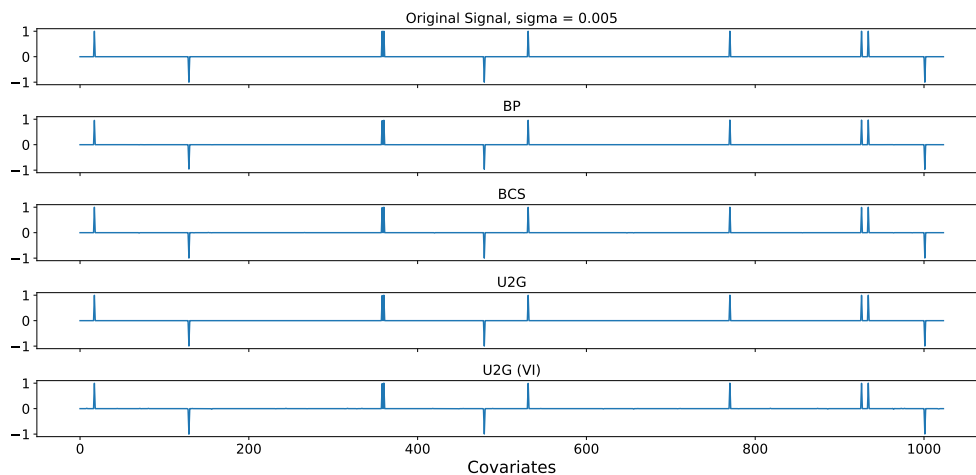


Figure 10: Results of compressive sensing when SNR_d is high, with $n = 500$, $p = 1024$, $\sigma = 0.005$.

Table 8: Results of compressive sensing when the SNR is high, with $n = 500$, $p = 1024$, $\sigma = 0.005$.

	Precision	Recall	F1	Nonzero	RR	RTE	PVE
BP	0.009	1.000	0.019	1024	1e-3	508.0	0.9987
BCS	0.322	1.000	0.488	31	1e-4	55.4	0.9998
U2G	1.000	1.000	1.000	10	2e-5	9.2	1.0000
U2G(VI)	1.000	1.000	1.000	10	3e-5	13.7	1.0000